5. Results

5.1. Meteorology

5.1.1. The wind field

The primary data for this study include the continuous records of two or five minute averages at two stations established for this study. The first step in the analysis consisted of obtaining the resultant values of the wind records. That is, the records of wind speed and directions were used to obtain the corresponding vector **V** = *u***i** + *v***j**, where *u* and *v* are, respectively, from west and south components of the two or five minute interval wind observed at a given time and **i** and **j** are the unit vectors. The resultant component in a particular direction is equal to the arithmetic sum of respective components divided by the number of readings. Finally, the resultant, or vector mean, is obtained by reconverting resultant components into a single vector. The use of mean vectors for each half an hour or hour of a day reduces perturbations due to changes of the large scale winds or random disturbances to a level that is acceptable for the envisaged variations.

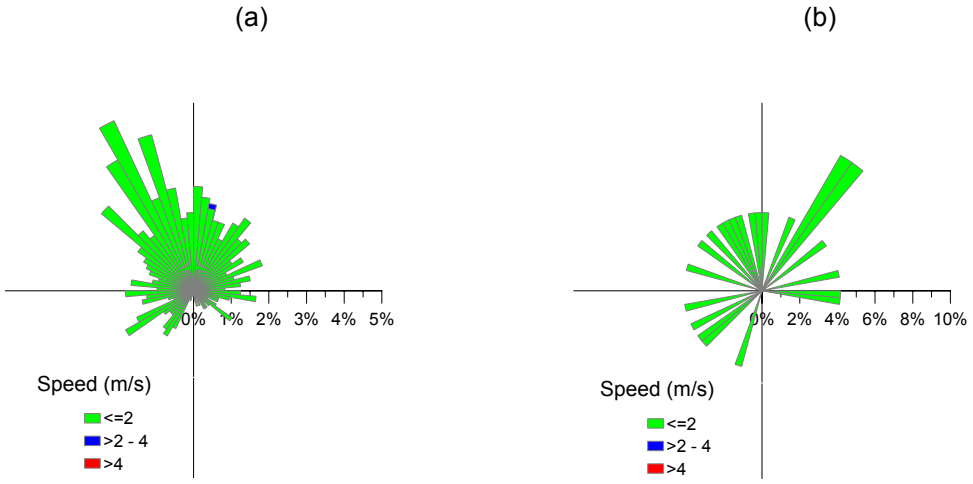

Figure 5.1. Wind roses for 27 March 2004 at Fura station obtained from: (a) 2 min interval records; and (b) derived hourly resultant winds.

Resultant wind has a value different from zero when there is either a preference for a given direction during the averaging time or there is a tendency for higher speeds for a certain direction. As an example of good representation of the hourly resultants, wind roses for variable light winds observed on 27 March 2004 were compared at Fura (Figure 5.1). The wind from three quadrants persisted nearly equally on the average. The hourly mean winds for 20 hours of the day have separate bins, with two bins in the NE representing more persisting winds during the recorded hours. More detailed examination of the wind roses revealed that the rare wind from SE quadrant is easily identified in both representations of the wind field.

5.1.1.1. Diurnal variation of the wind

In order to obtain a more detailed understanding of the general nature of the diurnal wind pattern along the western shoreline, half-hourly averages of 53 individual days (between 7 February and 30 March, 2004) were computed from 2 minute interval records of wind speed and direction. Resultant winds at half an hour intervals are considered to capture the observed short period oscillations. The half-hourly averaging period is centred at the beginning of each hour; for example, 0800 to 0828 for the 0800 value and 0830 to 0858 for the 0830 value. The orientation of the shoreline is such that fully developed lake-breeze comes from SE quadrant at both stations. A descriptive analysis of the diurnal changes in wind structure during this period is presented in the following paragraphs.

A detailed examination of observational data for the 53 days provided that the lake-breeze was observed daily at both stations. Figure 5.2 presents the relative frequency of the time when the lake-breeze started at Fura and Wajifo during the 53 days observations. At Wajifo, the lake-breeze started between 0730 and 0930 Local Standard Time (LST), predominantly around 0800 LST (about 60% of the time). The persistence of the lake-breeze is at least for 8 hours except for two days when the duration was only for 2.5 and 4 hours. Lake-breeze developed with NNE sector dominating during onset, and rotated clockwise to the SE quadrant within the next hour. The onshore wind speed increases rapidly before noon, mid-afternoon speeds falling close together. The most important feature of the resultant wind vector is that on individual days there is a strong tendency to turn counterclockwise during the onset of lake-breeze in the morning. Wind vectors turned in a clockwise direction in the remaining hours of individual days. The lake-breeze is followed by the variable wind, and before midnight a weak land breeze begins. The wind continues from the NW quadrant at less than 3 ms^{-1} through the early morning hours; but during the hour immediately preceding the lake-breeze, the wind is again variable. The lake-breeze caries average speed of 0.22–1.48 ms^{-1} in the first half an hour, increasing to 0.84–4.97 ms^{-1} in the next 2.5 to 9 hours.

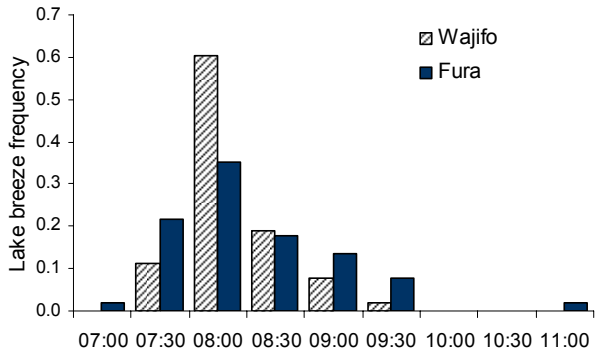

Figure 5.2. Observed lake-breeze starting time and frequencies at Wajifo and Fura stations from 07 February through 30 March 2004.

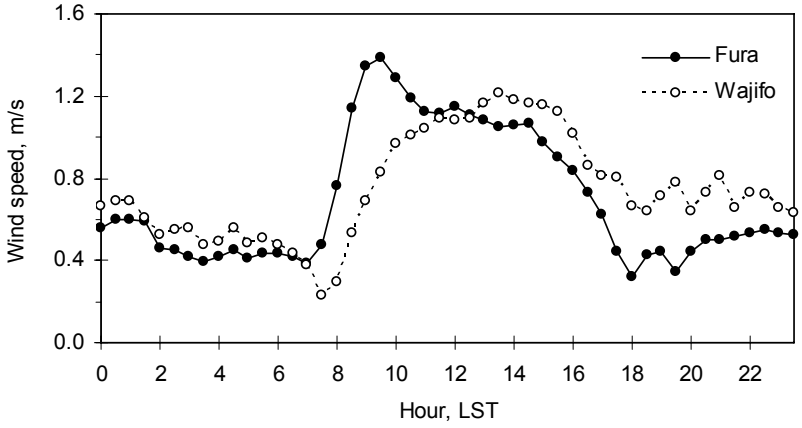

Figure 5.3. Average diurnal variation of wind speed at Fura and Wajifo stations for 53 days (from 07 February through 30 March, 2004).

A more detailed investigation of the diurnal wind variations for individual days revealed that erratic day-to-day changes of the half-hourly mean wind speeds at both stations. At Wajifo, winds fall off in strength during the night, reaching a maximum at various hours between 1000 and 1800 (all times in Local Standard Time) predominantly (for about 75% of the time). Maximum easterly winds occurred on 28 days between 0930 and 1330, on 13 days between 1430 and 1800, on 11 days between 1900 and 0030, and one day at 0830. Maximum westerly component occurred on 32 days between 1830 and 2330, on 16 days between 0030 and 0530, and on one day at 0730, 1330, 1430, 1630, and 1730. Maximum northerly winds occur on 22 days between 2200 and 0130, on 17 days between 1930 and 2100, on 8 days between 0230 and 0700, on 2 days at 0800, and one day at 1330, 1430, 1730 and 1830. Maximum southerly winds occur on 43 days between 1000 and 1800, on 7 days between 2100 and 0100, and one day at 0400, 1900 and 1930. Maximum winds from the south are much stronger than in the opposite direction from the north. Similarly, the easterly maximum wind components are stronger than westerly components. A definite stagnation occurs during the early morning and late afternoon hours before the lake-breeze begins and shifts to land breeze. The outstanding features of the diurnal wind on individual days at Wajifo are the high resultant speeds persisting on SE quadrant with little variation in direction after the lake-breeze developed around midmorning.

At Fura in the south, the first lake-breeze observed between 0700 and 1100 (Figure 5.2), predominantly being between 0730 and 0830 (about 75% of the time). The persisting large scale wind in the direction of the lake-breeze overlapped on two days and obscured the identification of the first observations. The persistence of the onshore wind is between 6.5 and 11.5 hours. Wind occurred on the SW quadrant on 29 days, on SE quadrant on 10 days, and 14 days on NE quadrant during onset. Variable wind during onset rotated clockwise direction on 15 days, turned in a counterclockwise direction on 38 days. The resultant wind carries an average speed in the range of 0.05 and 2.76 ms^{-1} in the next half an hour, which increases to 1.28 or 3.25 ms^{-1} between the next 1.5 and 6.5 hour. At the late hours when the onshore wind wanes, winds rotated in clockwise direction on 46 days

and showed tendency to turn counterclockwise on 7 days. Nighttime wind speeds are weak and close together.

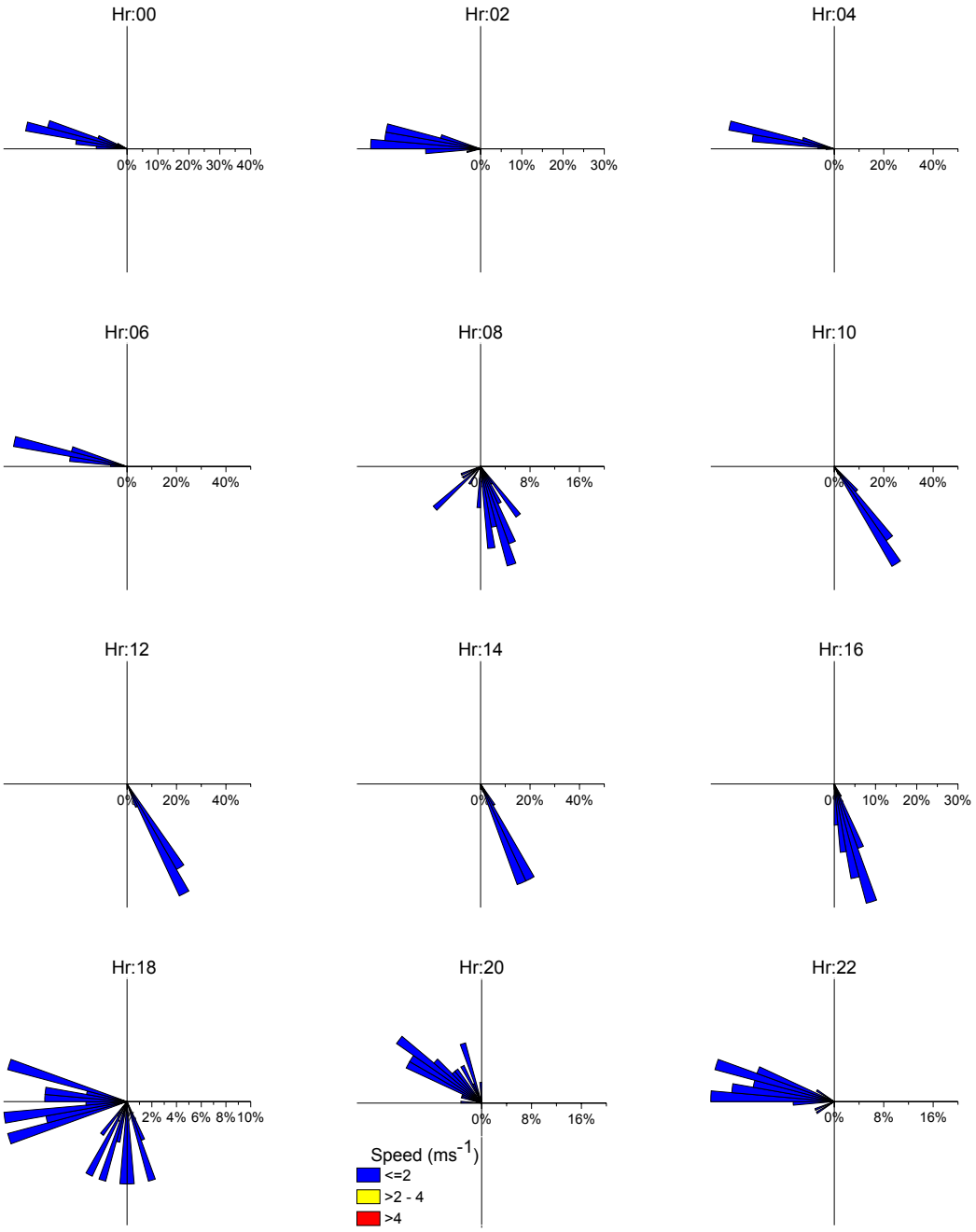

Figure 5.4. Wind roses at Wajifo station, 07 February–30 March 2004.

The diurnal variation of arithmetic mean wind speed at Fura and Wajifo stations is shown in Figure 5.3. It is shown that daytime portion of both curves is different from the nighttime portion. Furthermore, the average wind speeds rise rapidly between 0700 and 1000, relatively steady between 1200 and 1600, and fluctuate more between 1800 and 2100 LST.

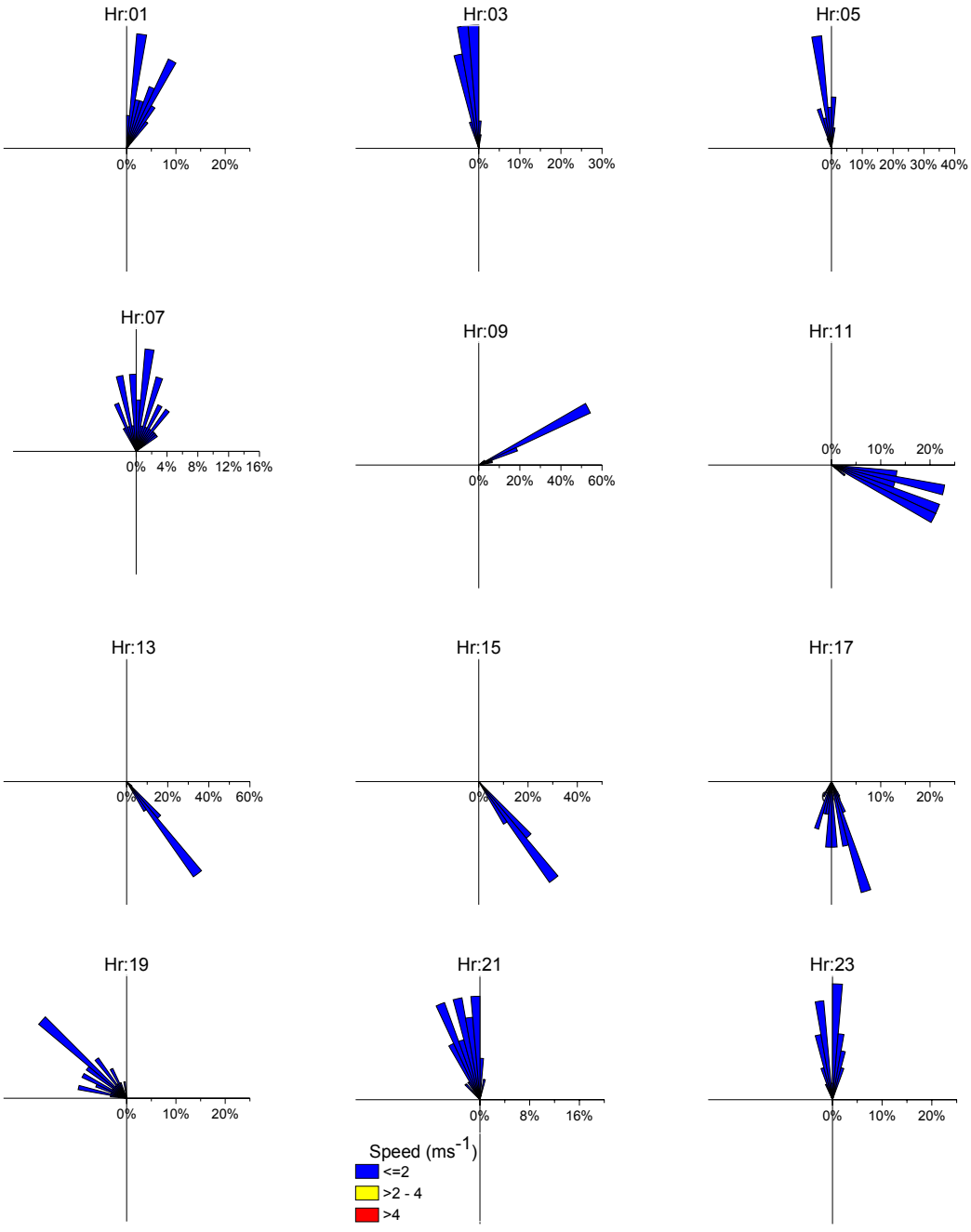

Figure 5.5. Wind roses at Fura Station, 07 February–30 March 2004.

The frequency of occurrence of maximum half-hourly average wind components on individual days is found to be more erratic at Fura. Maximum easterly winds occurred on 27 days between 0800 and 1000, on 12 days between 1030 and 1400, and on 10 days between 2030 and 0130. Maximum westerly component occurred on 21 days between 1900 and 2230, on 13 days between 0030 and 0300, on 9 days between 0430 and 0830, and on 7 days between 1630 and 1830. Maximum northerly winds occurred on 22 days between 0800 and 1000, on 14 days between 2200 and 0030, on 9 days between 0100

and 0600, and on 6 days between 1830 and 2100. Maximum southerly winds occurred on 39 days between 1230 and 1430, on 7 days between 1500 and 1700, and on 5 days between 1900 and 0030. Maximum winds from the south are much stronger than from the north, like in Wajifo. Similarly, the easterly maximum wind components are much stronger than westerly components in the opposite direction.

Figures 5.4 and 5.5 contain hourly wind roses for Wajifo and Fura for the resultant winds of 53 days. The two minute interval records were averaged over the 53 days of March and April 2004 to obtain the mean wind vector for each observation time at the stations. At Wajifo, the resultant winds are predominantly from the west and southeast with a rather distinct diurnal variation in speed. Winds are lighter during the night and the onshore wind increases rapidly until midmorning, reaches a maximum early afternoon, and then returns to a lower value around 1800 LST. Generally lower resultant velocities occur in the early morning hours and between hours of 1800 and 2000. Wind speeds between noon and mid afternoon, and between 0300 and 0600 LST tend to fall close together.

The fluctuation of wind speed and direction at 0800 and 1800 LST clearly marks the onset of lake-breeze and land breeze, respectively. The outstanding features of the wind roses for Wajifo are the counterclockwise rotation of the wind vectors during onset of lake-breeze and little variation in direction after midmorning. Rotation of the resultant winds is clockwise during daytime and onset of land breeze. There is a great tendency to veer and back alternatively before midnight. The resultant directional change between 0700 and 0800 LST and between 1800 and 2300 LST (limits included) are greater than the remaining hours of the 24-hr period.

The resultant winds at Fura (Figure 5.4) show clockwise rotation before midnight and the tendency to veer and back after midnight. The onset of lake-breeze and land breeze were marked by increased oscillation of the wind vector at 0700 and between 1700 and 1800 LST. The wind field persisted in the ENE sector mostly between 0800 and 1000 LST, completely shifted to ESE sector at 1100 LST. There was a great tendency of the actual wind rotating clockwise throughout the 24-LST period at Fura. The average daytime wind speed increased steadily to the maximum at the midmorning, fluctuated between midmorning and early afternoon, and finally deteriorated to minimum at 1800 LST. There is a tendency, as at Wajifo, for nighttime wind speeds to fall close together. More diurnal directional changes observed at Fura than at Wajifo.

By way of summary, the diurnal winds for February and March 2004 indicate the following characteristics. During the 53 days observations, the lake-breeze was in general able to dominate at both stations the over-riding and ever-changing large-scale flow. Along the western shoreline of Lake Abaya, lake-breeze develops by one hour earlier in the southern basin than in the north. Wind roses for both stations show clockwise rotation, but Wajifo show definite counterclockwise rotation during onset of lake-breeze. The westerly winds rotate to northward when they exit Fura in the south during nighttime. At Wajifo, winds are generally westerly during nighttime and the north components are very light. Resultant winds are in the NE quadrant during some period of the day at Fura and become nearly parallel to winds at Wajifo later in the afternoon in the SE quadrant. It is noted that the rate of turning of the direction of the lake-breeze and land breeze is not uniform over a 24 hour period. Afternoon winds are found to rotate slightly in clockwise direction at both stations.

The directional changes to the reverse directions during the onset of lake-breeze at Wajifo and land breeze at Fura are abrupt. Time of maximum resultant wind is in the midmorning at Fura, but tends to be four hours later at Wajifo station. The light lake-breeze in the morning at Fura is partially distorted by changing large-scale flow pattern.

5.1.1.2. Monthly variability of wind field

Figures 5.6 and 5.7 present the statistics of monthly winds of 2 or 5 minutes records observed for one year from March 2004 to February 2005 at two stations situated at the west boundary of Lake Abaya. The observed wind speeds, u, are classified in three ranges ($u \leq 2ms^{-1}$, $2ms^{-1} < u \leq 4ms^{-1}$, $u > 4ms^{-1}$). The considerable difference between graphs of two stations corresponding to the same month obviously indicates the importance of the winds of local origin at a given site around the lake. On the other hand, remarkable similarities and differences between monthly wind roses at a station mark the presence of characteristic seasonal pattern.

The outstanding feature of the monthly wind roses at Wajifo (Figure 5.6) is that winds showed strong directional preference. A persistent southeast wind occurred throughout the year (23-47% of the monthly period), but is most prominent during the period approximately from May through July 2004 (36-47% of the monthly period). Little directional change noted in the SSE sector from May through June and October through December 2004, when winds were stronger for significant portions of these months. Westerly winds observed continuously, being nearly at right angle to the SE winds. From March through April 2004, westerly winds occurred predominantly. Southeasterly and westerly winds were nearly equally important from September through October 2004 and from January through February 2005. Generally, southeasterly winds are stronger than westerly winds, and winds from NE quadrant are rare.

Fura station experienced winds from different quadrants over a significant portion of the time (Figure 5.7). The northeasterly winds occurred only between 3-7% of the monthly periods from May through August 2004, during which southwesterly winds from opposite direction occurred predominantly. Northeasterly winds observed to be predominant over southwesterly counterparts in the reverse direction during the remaining months of the year considered in this study. Northwesterly winds occurred predominantly over southeasterly winds all the time, except February 2005 when winds in both direction were nearly equally important.

Next Figure 5.8 gives the speed class histograms for monthly winds in the ranges 0-2 ms^{-1}, 2-4 ms^{-1}, and exceeding 4 ms^{-1} for the months of calmest and highest wind speeds and the average of 12-month period at Wajifo and Fura stations. During the study period considered in this study the observed wind speeds were predominantly < 2 ms^{-1} (between 92 and 98% of the monthly periods at Fura, and between 62 and 95% at Wajifo). At Wajifo in the north, the moderate and strong winds occurred more frequently in June, but at Fura in the south December winds were in general stronger than any other month of the year considered. The maximum wind records in different months at Wajifo and Fura, respectively, were about 5.2–8.9 ms^{-1} and 3.9–6.5 ms^{-1}. The maximum recorded wind speed occurred on May 05, 2004 at 1810 LST at Wajifo and later at 2035 LST at Fura. Since the collected wind data were 2 or 5 minute interval records, the actual maximum

wind speed that occurred during the year may not have been captured although it would not be expected to differ greatly from the measurements. The calmest month was August at Fura and January at Wajifo (Figure 5.8) which had peak frequencies of occurrence in the 0-2 ms^{-1} bin.

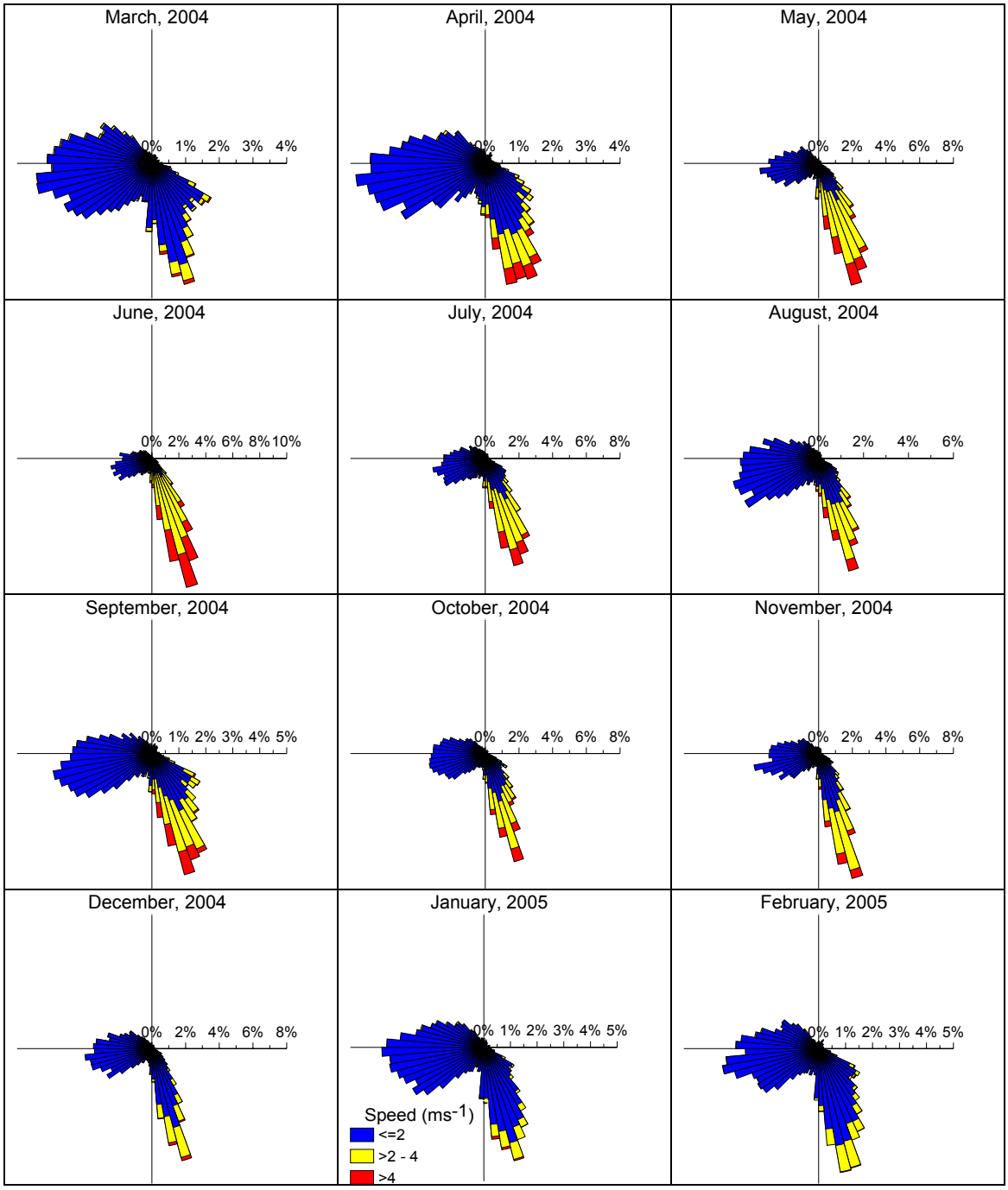

Figure 5.6. Monthly wind roses at Wajifo Station.

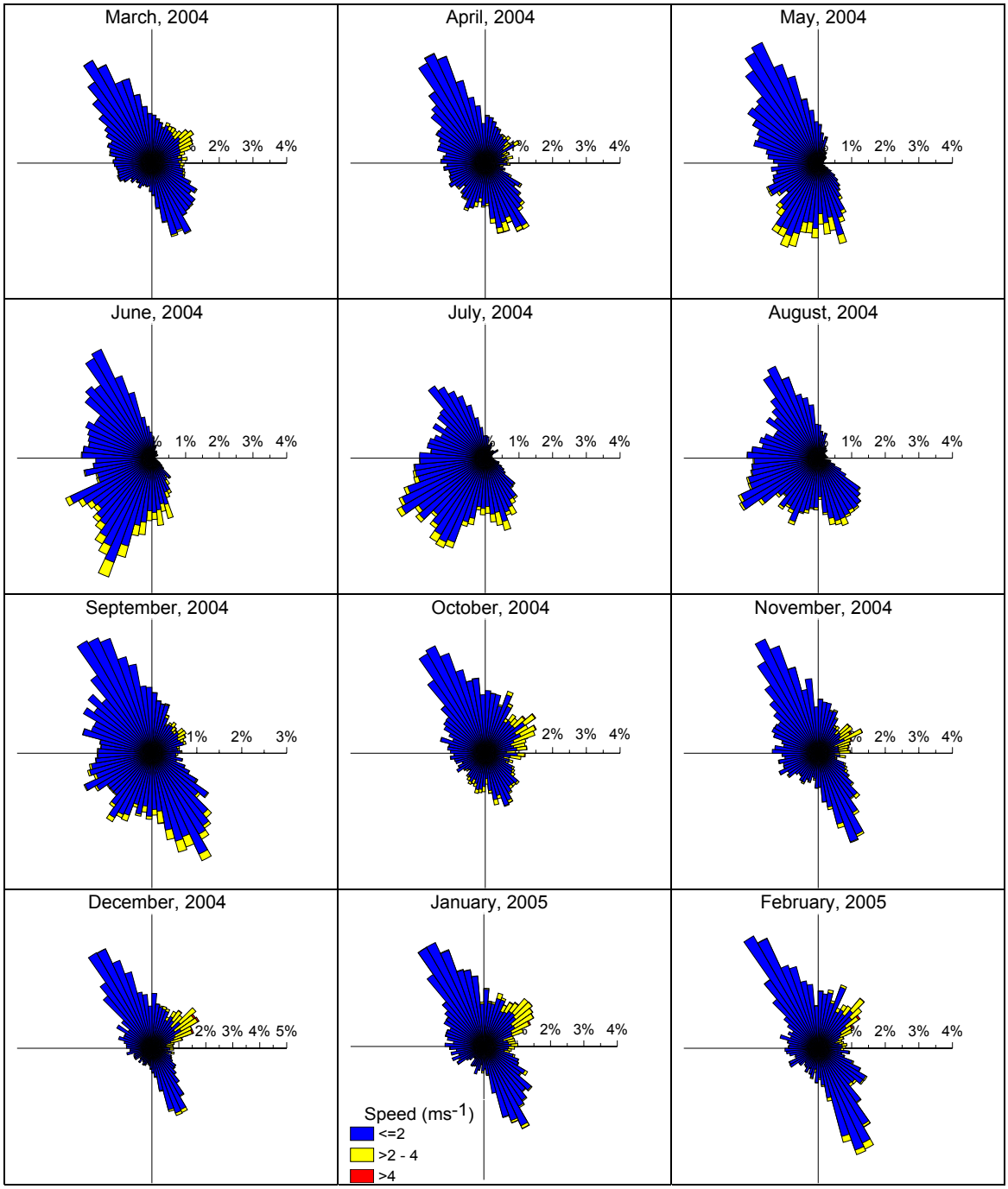

Figure 5.7. Monthly wind roses at Fura station.

5.1.1.3. Periodicity analysis

This section is concerned with periodic components that may contribute to measured wind. Spectra presenting the distribution of kinetic energy as a function of frequency are useful in picking out some of the more energetic oscillatory components (Saylor and Miller, 1987) in the wind speed records. To this end, the monthly spectra were estimated from hourly average speed along dominant directions for both stations in units of wind speed squared per cycle per hour. The dominant directions were identified for each month from wind roses

(Figures 5.6 and 5.7) and wind direction histograms, but not reported here. Observed spectra have very similar shapes, and typical spectral plots of for two months are shown in Figure 5.9.

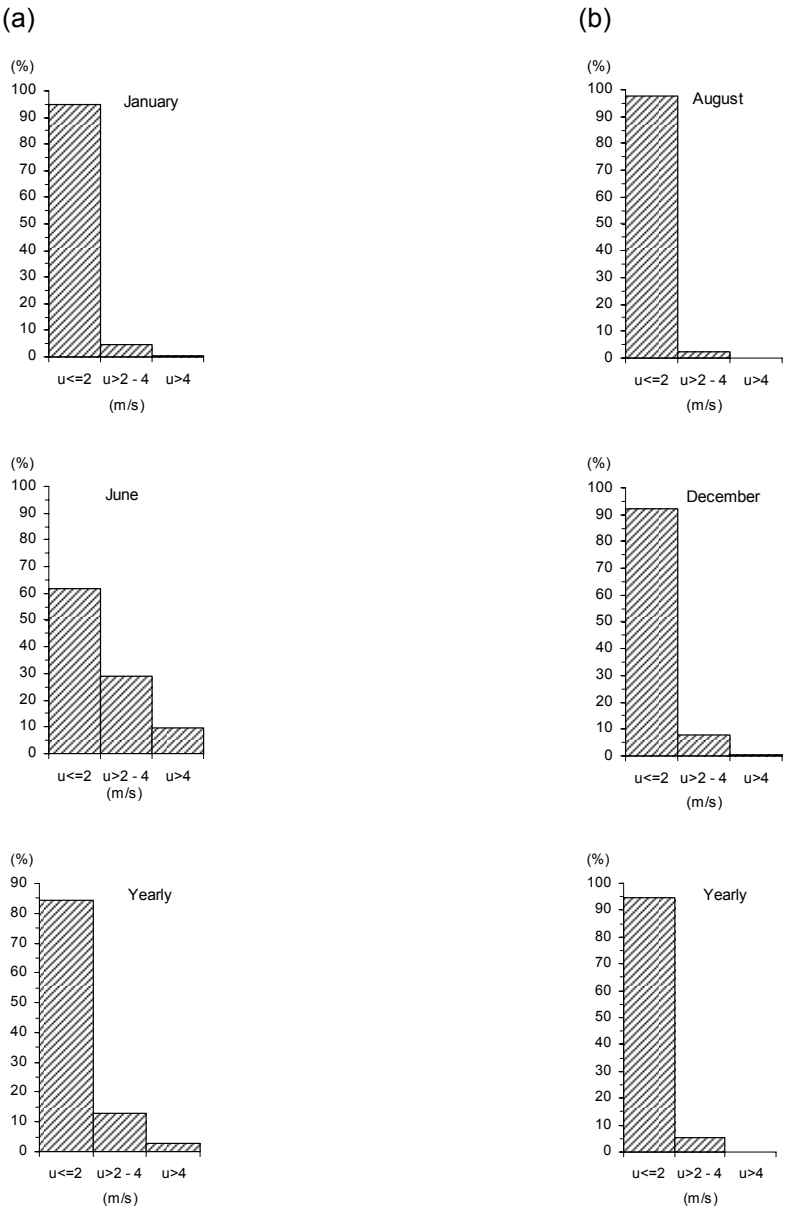

Figure 5.8. Speed class histograms at Wajifo (a), and Fura (b) stations during calmest (top), strongest (middle) and yearly average (bottom).

All spectra indicate pronounced peak at about 0.0417 cycle per hour (cph) frequency, which corresponds to a period of 1 day (the diurnal frequency). The magnitude of this peak is higher at Fura across-shore in all months, except July and August 2004. At Wajifo, the magnitude of the spectra peak at diurnal frequency appeared higher for across-shore wind component than along-shore component of the wind in all months, except in March, April and August 2004. Another remarkable feature from monthly spectral estimates is that the

energy distribution is in general broader across-shore component at Wajifo and along-shore component at Fura. Thus the estimated power spectra of wind speed in the frequency range between 0 and 0.5 cph fall into two more or less distinct groups depending upon the broadness of the energy distribution as shown in Figure 5.9. It should be noted that the only significant periodicity contained in the spectra, in the frequency interval between 0 and 0.5 cph, is that associated with the diurnal oscillations, as evidenced by the sharpness of the peak and its harmonics. Furthermore, most of the spectral energy at both stations is concentrated in the across shore direction, as suggested by the wind roses.

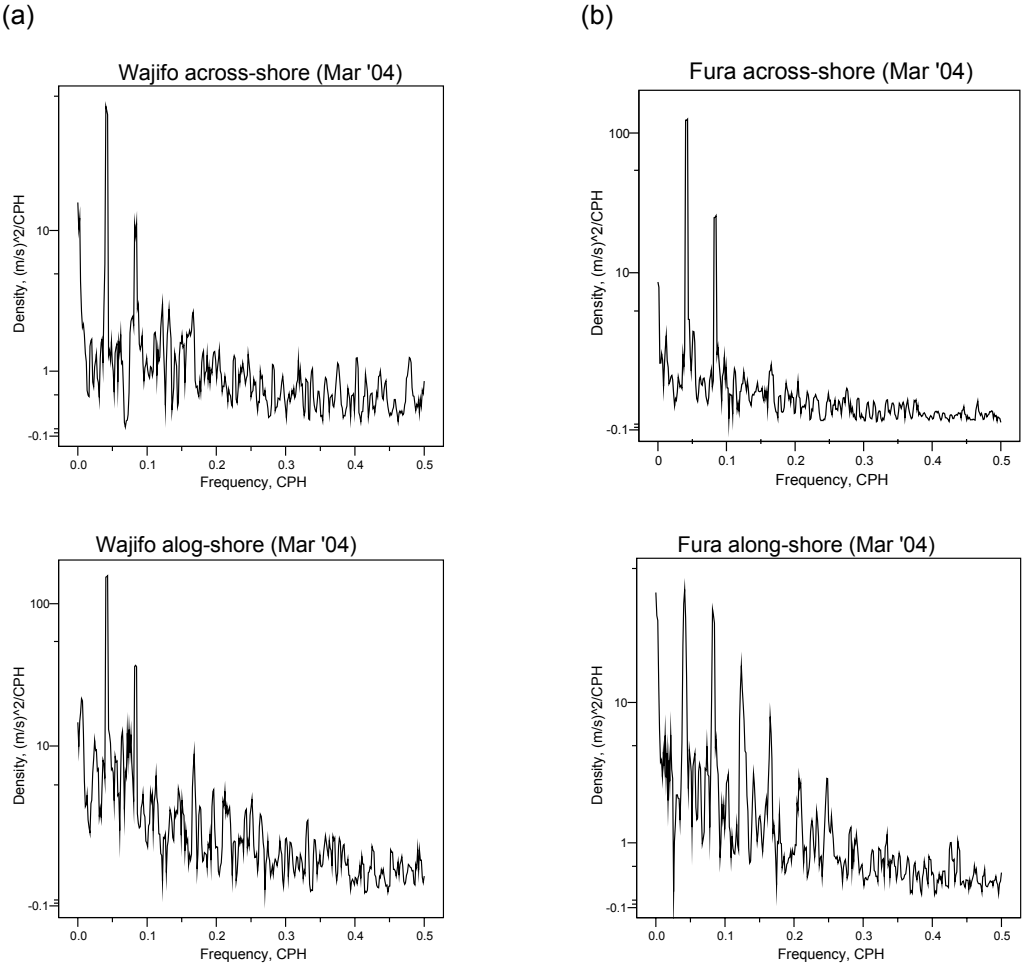

Figure 5.9. Typical monthly spectra of the two components of the wind vector at two stations.

5.1.2. Temperature

Frequency distributions of hourly temperatures at Wajifo station (Figure 5.10) from March 2004 through February 2005 have been analysed in order to obtain detailed information as to what actual temperatures encountered during the months. Five minute interval records are the bases of all temperature data: the hourly mean is defined as the average of 12 values. Averaging by individual hours enables us to establish the average daily march of

the temperature. Similarly, the daily means are computed as arithmetic means of 24 hourly means derived from 5 minutes interval records mentioned above.

Figure 5.10 presents the frequency distribution histograms of hourly temperatures using totals for each month. Here the problem to be investigated concerned the distribution of hourly temperature, regardless of the time of occurrence. Six temperature ranges distinguished (≤ 10^{o}C, >10-15^{o}C, >15-20^{o}C, >20-25^{o}C, >25-30^{o}C, > 30^{o}C). Plots for each month are easily compared by observing the relative frequency of temperature ranges. These show considerable month-to-month variability in the temperature regime at Wajifo. The hourly temperatures were predominantly >20^{o}C, (about 70-80% of the monthly hours).

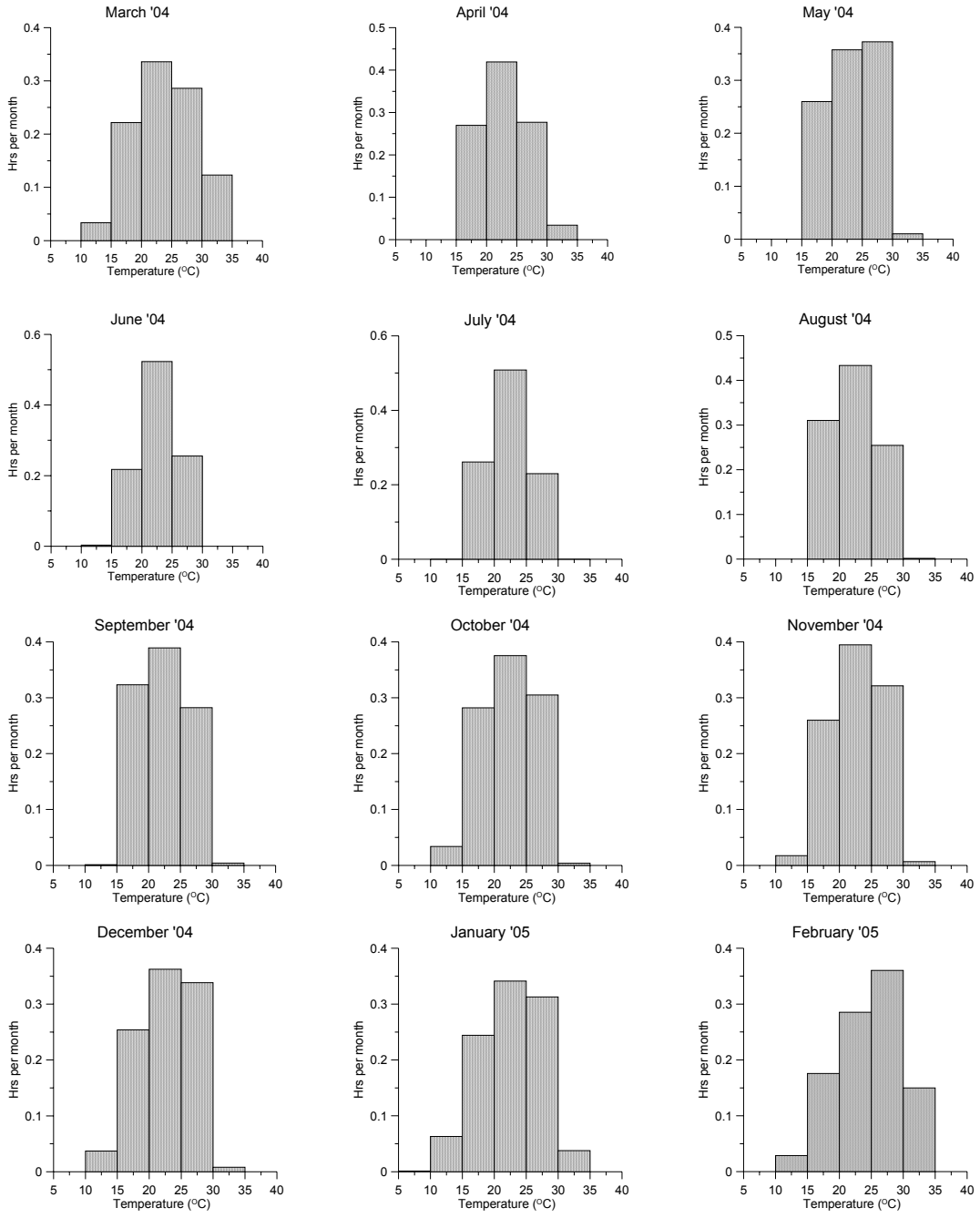

Figure 5.10. Monthly hourly average temperature frequencies at Wajifo Station.

Another marked feature in the temperature class histograms is the larger variability in March 2004 and from January through February 2005, and the smaller in July through September 2004. A third remarkable feature occurred in January and February 2005, respectively, where the coldest month (the hourly average temperature was < 15^{o}C, for about 6% of the time) was fallowed by warmest month (the hourly temperatures were >30% for about 15% of monthly hours). The hourly average temperature gradient reached its maximum in August 2004.

Table 5.1. Descriptive statistics of hourly average temperature in different months from March 2004 to February 2005 at Wajifo.

Month	n	Range	Minimum	Maximum	Mean	St. Dev	Skewness
Mar '04	744	14.3	12.2	35.3	23.8	4.937	0.004
Apr '04	720	10.5	17.1	31.5	23.0	3.647	0.423
May '04	744	10.2	16.8	31.4	23.3	3.598	0.060
Jun '04	720	8.6	14.7	28.8	22.6	2.896	-0.159
Jul '04	744	9.3	15.3	29.3	22.4	3.074	0.149
Aug '04	744	9.6	16.4	29.8	22.4	3.360	0.391
Sep '04	720	10.6	15.1	30.4	22.5	3.560	0.247
Oct '04	744	12.1	12	29.9	22.5	4.089	-0.124
Nov '04	720	11.6	12.2	30.5	22.8	3.835	-0.160
Dec '04	744	12.7	10.9	31.7	22.7	4.256	-0.207
Jan '05	744	13.4	10	31.4	22.7	4.746	-0.288
Feb '05	672	14.8	12.7	35.1	24.5	4.797	-0.280

It is of interest to investigate the descriptive statistics were computed for monthly totals (Table 5.1) to obtain further information on the hourly temperatures variations during the year considered in this study. The annual mean temperature at Wajifo station was 22.9^{o}C. Monthly variations in standard deviations found to be in good agreement with corresponding variations in the customary index of temperature, the mean daily range. The greatest average daily range of the year occurred in the warmest month of the year January 2005, while the least daily range averaged to 3^{o}C in July 2004. A second general feature is that skewness of the monthly totals tended to be equally positive and negative during the year considered, but the differences from the normal are minor in general. The largest positive skewness and largest monthly minimum noted in April 2004, whereas a large negative skewness and a small monthly mean observed in January 005.

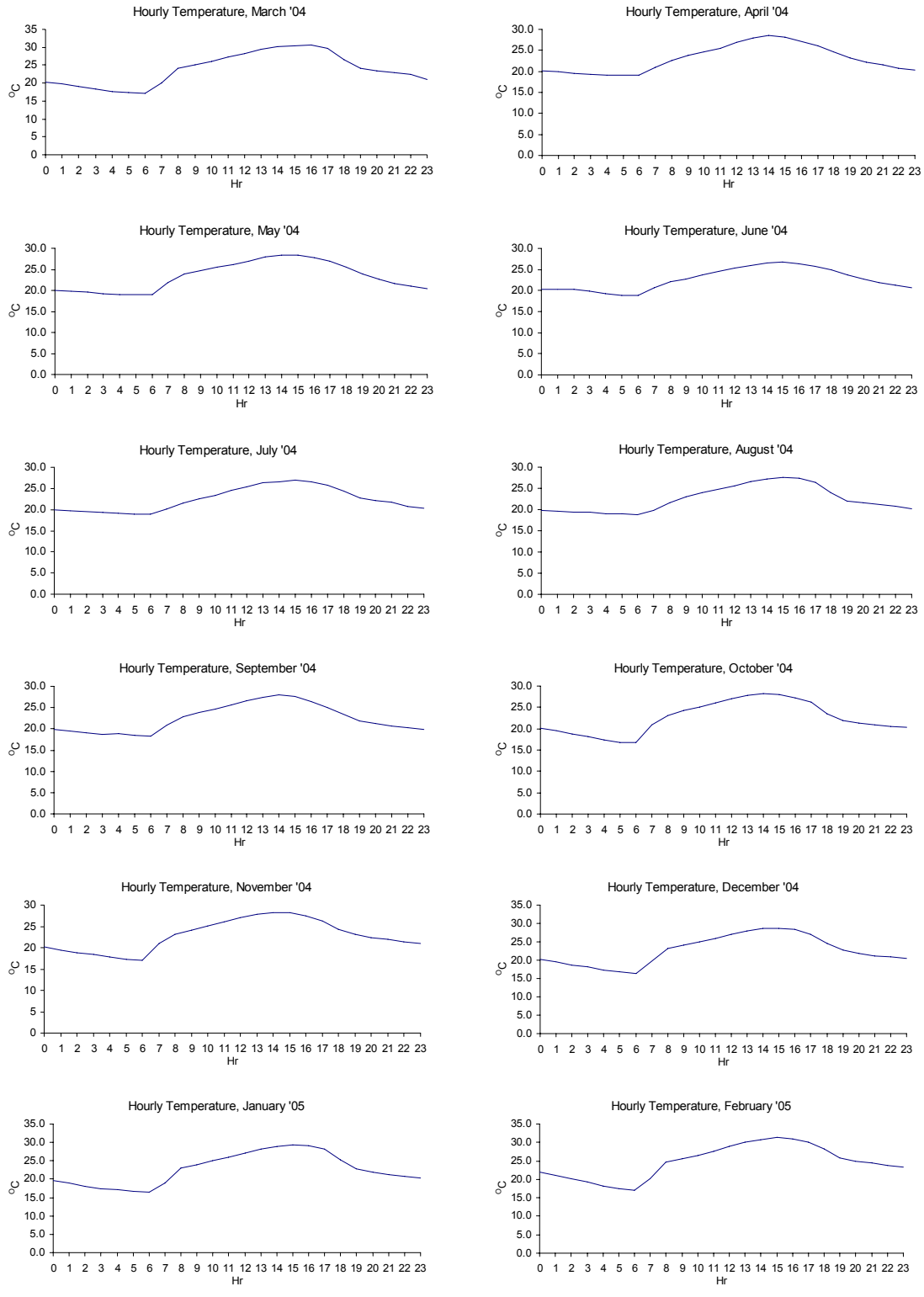

Figure 5.11. Diurnal variability of temperature at Wajifo Station.

5.1.2.1. Diurnal variability of temperature

As an indicator of human comfort, and also for purpose of applied climatology, it is important to know what percentage of the time various temperature are exceeded (at the earth's surface) during particular months at a given location (Spreen, 1956). Next in Figure 5.11 are shown the average values of air temperature, by hour of the day, for each month separately. The average 24 hourly values of a month are obtained as simple arithmetic means of the particular hours of an entire month. The resulting monthly averages over individual hours appear to be much more smoothened than would be expected from the hourly averages of daily observation considered alone. Nonetheless, close inspection of individual graphs shows systematic changes of the hourly variation of mean temperature. From 0600 to 0800 LST, rapid rise on the average appeared in all months, except from June through August 2004. Notice that maximum rise from 0600 to 0800 LST by 7.6^{o}C noted for February 2005, minimum rise by 2.6^{o}C for July 2004. The average traces show the temperature maximum oscillating during the period from 1400 to 1600 LST. In general, regular increase in temperature observed from 0800 LST to the period of maximum temperature, followed by a mean temperature drop of less than 1 ^{o}C on the next hour.

5.1.2.2. Interdiurnal variability of temperature

The discussions in the previous section about the range of variability of temperature considered the variations to which the average values are subjected. The task of this section is to investigate the variations from day to day. These are called interdiurnal variability (or IDV), and computed as the difference between either the daily mean or a fixed hour of a day and that of the next day (Conrad, 1947). Increasing temperature from one day to the next is called "warming", decreasing "cooling" (Conrad, 1942). Using these definitions the interdiurnal variability is computed for a daily averages and extremes for a time which lies close to the daily minimum on the one hand and to the daily maximum on the other hand.

Tables 5.2 and 5.3 show the interdiurnal variability of daily average temperature at Wajifo station. The primary modes of the frequency distributions of interdiurnal variability of warming tend to persist in the 0-1^{o}C class interval throughout the year. On the other hand, two noticeable exceptions observed for the persistence of the primary modes in the 0-1^{o}C class interval of interdiurnal variability of cooling frequency distribution during April and October 2004. Another remarkable fact to be noted is that the variability of cooling is found to exceed warming, except for May and November 2004 where they were nearly equally variable.

Table 5.2. Percentage frequency of the various values of daily mean IDV of warming (^{o}C) at Wajifo

IDV	Mar	Apr	May	Jun	Jul	Aug	Sep	Oct	Nov	Dec	Jan '05	Feb
0 – 1	72.2	66.7	100.0	76.9	62.5	66.7	94.4	76.2	88.9	71.4	76.5	75.0
1 – 2	27.8	33.3	00.0	15.4	37.5	26.7	05.6	19.0	11.1	28.6	17.6	25.0
2 – 3	00.0	00.0		07.7	00.0	06.6	00.0	04.8	00.0	00.0	05.9	00.0
3 – 4				00.0		00.0		00.0			00.0	

Table 5.3. Percentage frequency of the various values of daily mean IDV of cooling (^{o}C) at Wajifo

IDV	Mar	Apr	May	Jun	Jul	Aug	Sep	Oct	Nov	Dec	Jan '05	Feb
0 – 1	61.5	33.4	100.0	82.4	73.3	68.8	75.0	40.0	91.7	82.4	78.6	75.0
1 – 2	15.4	50.0	00.0	11.8	20.0	12.5	16.7	50.0	08.3	17.6	14.3	16.7
2 – 3	07.7	08.3		05.8	06.7	18.8	08.3	10.0	00.0	00.0	00.0	08.3
3 – 4	15.4	08.3		00.0	00.0	00.0	00.0	00.0			07.1	00.0
4 – 5	00.0	00.0									00.0	

Next Tables 5.4 through 5.7 present frequencies of differences from day to day close to hours of extremes. The primary modes of frequency distributions of warming in the 0-1^{o}C and 1-2^{o}C class intervals are nearly equally important at 0600 LST, 0-1^{o}C being dominant at 1500 LST except for June and February when 1-2^{o}C class interval was more significant. The dominant mode for cooling throughout the year is in the 0-1^{o}C class interval, except in April and August 2004, when 1-2^{o}C class interval was more important. The interdiurnal variability of warming and cooling are nearly the same at 0600 LST. At 1500 hrs day to day difference of warming and cooling found to be higher from March through April 2004, July through September 2004 and February 2005. The greatest interdiurnal variability of daily average warming was 2.3^{o}C, while cooling was 3.5^{o}C; at 0600 LST the corresponding values for cooling and warming, respectively, were 4.7^{o}C and 6.1^{o}C, and at 1500 LST greatest warming 7.8^{o}C and cooling was 6.6^{o}C. Thus the observed ranges of interdiurnal variability are smaller for cooling than warming.

Table 5.4. Percentage frequency of the various values of 0600 LST IDV of warming (^{o}C) at Wajifo

IDV	Mar	Apr	May	Jun	Jul	Aug	Sep	Oct	Nov	Dec	Jan '05	Feb
0 – 1	60.0	37.5	35.7	20.0	43.8	46.2	46.6	53.8	50.0	25.0	41.2	33.3
1 – 2	13.3	37.5	57.1	33.3	31.2	38.5	26.7	15.4	06.2	33.3	23.5	33.3
2 – 3	00.0	18.8	07.2	20.0	25.0	00.0	26.7	23.1	31.3	16.7	23.5	33.3
3 – 4	13.3	06.2	00.0	20.0	00.0	15.3	00.0	07.7	12.5	16.7	00.0	00.0
4 – 5	00.0	00.0		00.0		00.0		00.0	00.0	08.3	05.9	
5 – 6	06.7			06.7						00.0	05.9	
6 - 7	06.7			00.0							00.0	
7 – 8	00.0											

Table 5.5. Percentage frequency of the various values of 0600 LST IDV of cooling (^{o}C) at Wajifo

IDV	Mar	Apr	May	Jun	Jul	Aug	Sep	Oct	Nov	Dec	Jan '05	Feb
0 – 1	62.5	57.1	64.7	20.0	40.0	66.6	40.0	44.4	50.0	36.8	50.0	53.8
1 – 2	12.5	21.3	23.5	33.3	33.3	16.7	33.3	44.4	07.2	31.6	14.3	38.5
2 – 3	06.2	07.2	05.9	33.3	06.7	16.7	26.7	05.6	35.6	26.3	07.2	00.0
3 – 4	18.8	07.2	00.0	13.4	20.0	00.0	00.0	05.6	07.2	05.3	21.3	07.7
4 – 5	00.0	07.2	05.9	00.0	00.0			00.0	00.0	00.0	07.2	00.0
5 – 6		00.0	00.0								00.0	

The annual marches of the average and extreme values for daily average, 0600 and 1500 LST are to be seen separately for warming and cooling in Table 5.8. Within one year period, the greatest warming was 7.8^{o}C and the greatest cooling was 6.6^{o}C. Overall, the variability was somewhat higher at 1500 LST than in the early morning. There seems slightly marked annual march of the interdiurnal variability at 1500 LST, with a high maximum in July through September and a deep minimum in November through January. Lack of marked annual march of the interdiurnal variability at 0500 LST and for daily averages is explained by the shortness of the period of only one year. It is remarkable to note that warmings are slightly greater than coolings from day to day at 0600 LST, while this relation is the reverse at 1500 LST and for daily averages.

Table 5.6. Percentage frequency of the various values of 1500 LST IDV of warming (^{o}C) at Wajifo

IDV	Mar	Apr	May	Jun	Jul	Aug	Sep	Oct	Nov	Dec	Jan '05	Feb
0 – 1	40.0	31.3	76.5	35.7	40.0	55.5	50.0	56.3	53.8	60.0	76.4	36.4
1 – 2	40.0	25.0	05.9	50.0	40.0	22.1	31.3	25.0	23.1	26.7	11.8	45.4
2 – 3	00.0	25.0	17.6	00.0	00.0	05.6	00.0	06.2	23.1	13.3	11.8	09.1
3 – 4	13.3	12.5	00.0	14.3	13.3	05.6	06.2	12.5	00.0	00.0	00.0	00.0
4 – 5	06.7	06.2		00.0	00.0	00.0	00.0	00.0				09.1
5 – 6	00.0	00.0			00.0	05.6	12.5					00.0
6 - 7					00.0	05.6	00.0					
7 – 8					06.7	00.0						
8 – 9					00.0							

Table 5.7. Percentage frequency of the various values of 1500 LST IDV of cooling (^{o}C) at Wajifo

IDV	Mar	Apr	May	Jun	Jul	Aug	Sep	Oct	Nov	Dec	Jan '05	Feb
0 – 1	56.3	21.4	71.4	43.8	43.8	30.8	35.7	66.7	47.1	75.0	71.4	47.1
1 – 2	18.8	35.7	07.2	31.2	25.0	46.1	28.6	13.2	41.2	06.2	21.4	41.1
2 – 3	06.2	14.3	14.2	18.8	18.8	00.0	07.2	06.7	11.7	18.8	07.2	00.0
3 – 4	06.2	21.4	07.2	06.2	06.2	07.7	21.3	06.7	00.0	00.0	00.0	05.9
4 – 5	00.0	07.2	00.0	00.0	06.2	07.7	00.0	06.7				00.0
5 – 6	00.0	00.0			00.0	00.0	00.0	00.0				05.9
6 - 7	12.5					07.7	07.2					00.0
7 – 8	00.0					00.0	00.0					

Table 5.8. Interdiurnal variability of temperature, ^{o}C, at Wajifo

Month	Warmings						Coolings					
	Average values			Maxima			Average values			Maxima		
	Daily	0600 hr	1500 hr	Daily	0600 hr	1500 hr	Daily	0600 hr	1500 hr	Daily	0600 hr	1500 hr
Mar	0.8	1.6	1.5	1.7	6.1	4.7	1.1	1.3	1.7	3.4	3.7	6.4
Apr	0.8	1.3	1.8	1.8	3.2	4.0	1.3	1.4	2.1	3.5	4.5	4.9
May	0.4	1.1	0.9	0.9	2.4	2.2	0.5	1.0	1.0	1.0	4.6	3.3
Jun	0.8	2.2	1.3	2.2	5.1	3.5	0.6	1.9	1.4	2.2	3.9	3.5
Jul	0.7	1.3	1.7	1.6	2.9	7.8	0.8	1.6	1.4	2.2	3.5	4.7
Aug	1.0	1.3	1.5	2.0	3.1	6.1	0.9	1.0	2.0	2.7	2.9	6.5
Sep	0.6	1.3	1.6	1.1	2.9	5.4	0.9	1.3	2.0	2.4	2.4	6.6
Oct	0.6	1.4	1.2	2.1	3.7	3.8	1.2	1.1	1.1	2.1	3.2	4.5
Nov	0.4	1.4	1.2	1.7	3.8	2.8	0.7	1.6	1.0	1.9	3.3	2.6
Dec	0.7	2.0	1.0	1.9	4.6	3.3	0.7	1.5	1.0	1.9	3.6	3.0
Jan	0.6	1.7	0.8	2.3	5.6	2.1	0.6	1.8	0.8	3.4	4.7	2.9
Feb	0.7	1.5	1.6	1.8	2.9	4.8	0.8	1.2	1.3	2.0	3.2	5.3
Yearly	0.7	1.5	1.3	1.8	3.9	4.2	0.8	1.4	1.4	2.4	3.6	4.5

5.1.3. Atmospheric pressure oscillation

The atmospheric pressure at any place is found to exhibit certain periodicities if averages are taken over a sufficiently long period of time. The best known of these periods are the diurnal, the semi-diurnal and the annual (Spar, 1950). In this section we shall consider one year records of surface observations of atmospheric pressure taken at 5-minute intervals at Wajifo station. Thus the basic data analysed here can hardly be regarded as adequate to represent the general atmospheric pressure oscillation.

In Figure 5.12 are shown monthly atmospheric pressure variations from which the mean has been eliminated. It is seen that the oscillations about the mean are stationary and the amplitude of the diurnal oscillation of the atmospheric pressure varies between 3.5 and 20.2 mb. It appears obvious at first sight that the fluctuations are mainly diurnal and semidiurnal, and larger amplitudes do not seem to occur more than a few days in the year considered in this study. The maximum hourly average atmospheric pressure value of about 891 mb was observed in September 2004, and the minimum value of about 873 mb was occurred in April 2004 and January 2005. The least and most extremes, respectively,

were observed in the consecutive months May and June 2004. The lowest pressure was occurred in August, and the highest was observed in June. The total pressure range observed during each month was found to be nearly the same for most portion of the year. The observed large pressure changes occurred over different time intervals. For, example, pressure change of 22 mb in November 2004 occurred after only 2 days. On the other hand in May, the minimum monthly change occurred after 9 and 15 days. On 1 January 2005, the maximum pressure was 988 mb, the highest over 1-year period, 13 days later the pressure had fallen by 118 mb to 871mb.

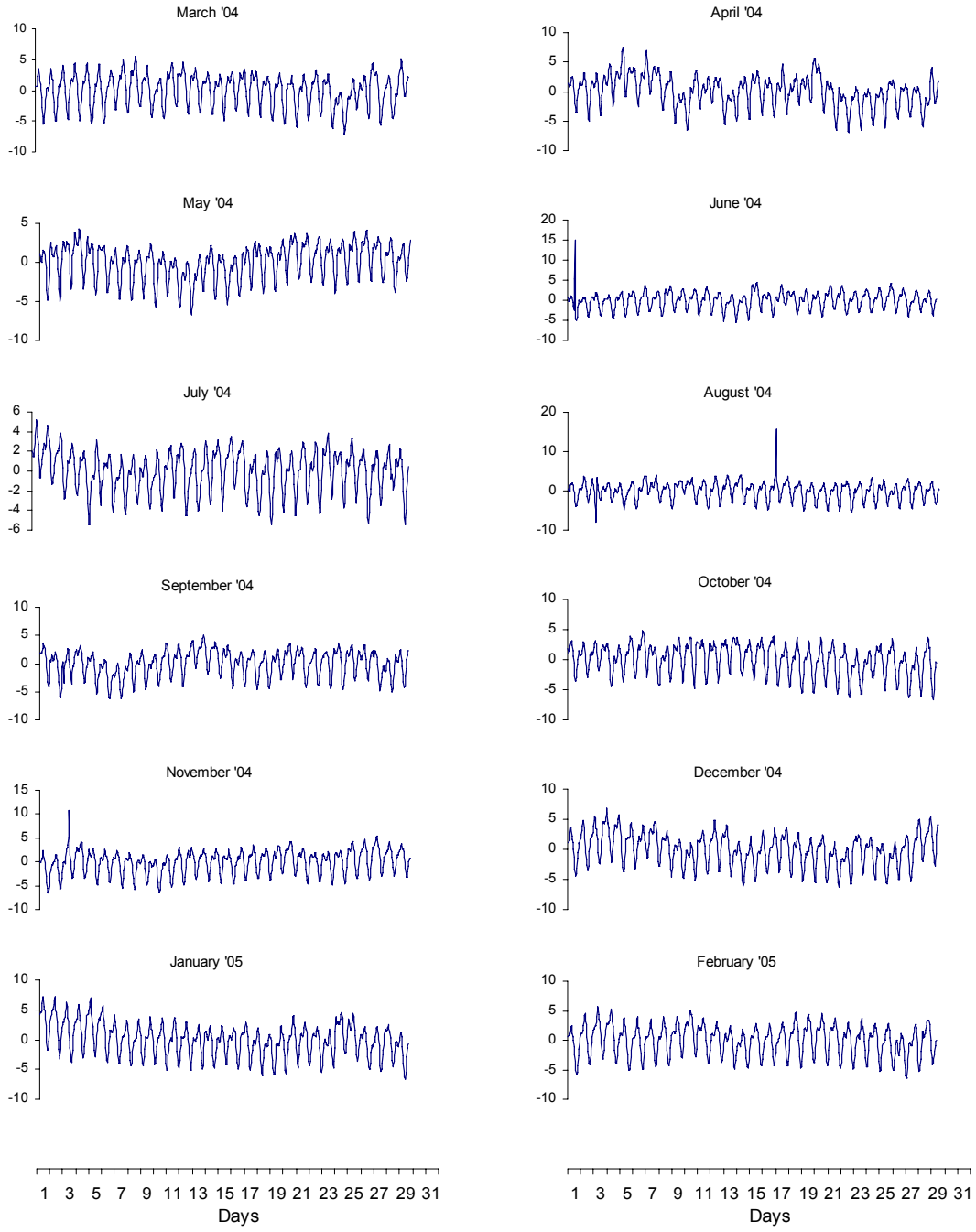

Figure 5.12. Atmospheric pressure oscillations from monthly mean at Wajifo Station.

Table 5.9. Mean monthly pressure (mb) and departures from the mean monthly pressures. * denotes maxima of Diurnal Variation of Mean Pressure (DVMP), ** denotes minima of DVMP. Time is in Local Standard Time (LST)

Time	Mar '04	Apr	May	Jun	Jul	Aug	Sep	Oct	Nov	Dec	Jan '05	Feb
00	1.30	1.20	1.24	0.90	0.82*	0.85	0.95	1.21	1.29	1.04	1.16*	0.92
01	1.03	0.78	0.88	0.63	0.65	0.58	0.78	0.98	1.10	0.91**	1.07	0.85
02	0.93**	0.53**	0.60**	0.46**	0.55**	0.48**	0.67**	0.98**	1.03**	0.92	1.00**	0.78**
03	1.12	0.57	0.70	0.52	0.66	0.52	0.83	1.19	1.16	1.03	1.15	1.03
04	1.60	0.91	1.03	0.84	0.99	0.88	1.21	1.58	1.54	1.48	1.65	1.58
05	2.18	1.39	1.57	1.42	1.51	1.38	1.66	2.17	2.15	2.16	2.31	2.33
06	2.84	1.90	2.13	2.04	2.02	1.83	2.27	2.89*	2.82*	2.91	3.00	3.13
07	3.19*	2.33	2.28*	2.33*	2.41	2.26	2.46*	2.71	2.67	3.06*	3.41*	3.52*
08	2.56	2.37*	2.03	2.28	2.43*	2.37	2.25	2.14	2.35	2.34	2.64	2.55
09	2.25	2.09	1.85	2.19	2.27	2.80*	2.05	1.89	1.87	1.92	2.21	2.35
10	1.70	1.64	1.34	1.78	1.89	1.96	1.56	1.25	1.26	1.28	1.65	1.87
11	0.67	0.79	0.64	1.03	1.07	1.24	0.66	0.20	0.24	0.27	0.64	0.92
12	-0.56	-0.46	-0.39	0.04	0.14	0.23	-0.58	-1.08	-1.10	-0.95	-0.64	-0.37
13	-1.85	-1.89	-1.63	-0.78	-0.98	-0.98	-2.04	-2.38	-2.42	-2.19	-1.99	-1.77
14	-3.09	-3.16	-2.80	-1.55	-2.04	-2.19	-3.26	-3.47	-3.54	-3.36	-3.28	-3.06
15	-3.99	-3.89**	-3.69	-3.17	-3.03	-3.25	-3.80**	-4.17**	-4.22	-4.13	-4.17	-4.08
16	-4.42**	-3.86	-3.91**	-3.64**	-3.59**	-3.83**	-3.74	-4.15	-4.27**	-4.28**	-4.48**	-4.47**
17	-4.23	-3.27	-3.32	-3.41	-3.40	-3.65	-3.12	-3.55	-3.58	-3.71	-4.17	-4.24
18	-3.24	-2.30	-2.41	-2.73	-2.66	-2.80	-2.22	-2.34	-2.41	-2.56	-3.06	-3.31
19	-1.81	-1.16	-1.28	-1.80	-1.80	-1.66	-1.11	-1.12	-1.04	-1.18	-1.71	-1.92
20	-0.66	-0.17	-0.23	-0.88	-0.96	-0.82	-0.18	-0.10	0.02	0.00	-0.57	-0.69
21	0.25	0.78	0.69	0.00	-0.17	0.10	0.58	0.71	0.74	0.78	0.40	0.27
22	0.91	1.39	1.21	0.58	0.45	0.76	1.05	1.15	1.09	1.10	0.83	0.86
23	1.32*	1.46*	1.46*	0.93*	0.79	0.94*	1.07*	1.31*	1.27*	1.16*	0.93	0.97*
Mean monthly pressure	873.31	873.69	874.09	876.32	874.76	875.15	873.99	874.25	873.58	873.18	873.58	872.33

5.1.3.1. Daily variation of mean atmospheric pressure

Table 5.9 shows month-to-month changes of the daily variation of mean pressure. The data were organized in the form of 1-hr mean pressures for each individual month of the study period. Hourly means are centred at the start of the hour. To obtain a grand mean for

a particular hour and particular month, say 0000 LST local time for March, each of the particular hourly means of the days was added together and divided by the total number of days in the month.

The times of maxima and minima wander, in apparently nearly systematic fashion, from hour to hour during the course of the year. A detailed examination of the data shows that double structure appeared in all months, February 2005 showing larger departure from the mean monthly pressures. The morning primary maxima appeared between 0600 and 0900 LST: at 0600 LST in two months, at 0700 LST in seven months, at 0800 LST in two months and only in one month at 0900 LST. Afternoon primary minima found at 1500 LST in three months and at 1600 LST during the rest 9 months. Secondary maxima in the evening occurred at 2300 LST in nine months, at 0000 LST during the remaining three months. All months, except December, displayed the secondary minima at 0200 LST.

5.2. Sedimentology

5.2.1. Sediment distribution

Four major units of surficial sediment deposits of Lake Abaya were recognized: (1) silty-sand; (2) clayey-sandy-silt; (3) sandy-silty-clay; and (4) silty-clay. These divisions are based on in situ visual inspection of the fresh samples and are used in this study. Most of the sediments of Lake Abaya consist of silty clay; pure sand rarely lies at the mouth of main rivers near shore; yet most sand also contains silt and clay in significant amount. A comprehensive map of sediment distribution constructed based on visual description of sediment samples is shown in Figure 5.14. The distribution pattern is basically simple with a natural sorting of sediment units reflecting the different energy-regimes of the lake. Figure 5.14 demonstrates the courser nature of sediments near the mouth of the major rivers as well as exposed shallow regions parallel to the shorelines. The nearshore sediments are characterized by the high sand contents.

The general bathymetry of the lake is shown in Figure 5.13. The main basins are generally slop gently or flat bottomed and the shore areas usually have steep slope. The north basin is relatively more flat-bottomed and shallower with maximum observed depth of about 14 m, whereas the maximum water depth measured in the south basin is about 20 m, decreasing towards the east.

In shallow areas, particularly in the northernmost of the lake at Bilate River delta, the sand silt deposit extended southward. Marked increase in the sand population of samples taken near the mouth of major tributaries and the narrow passage between Gidicho Island and east shoreline in the north basin suggests a possible higher energy environment. This shows that the regions displaying the best-sorted sediments confined to nearshore zones, essentially to the mouth of the rivers in association with courser sediment, though some samples from deep and with hilly surrounding topography show a high fine material content. Regions of highest energy in the lake, occurs around the periphery of the lake in the nearshore zone. It is interesting that this zone predominates in the northern and eastern shores of the lake and is absent from regions with hilly surrounding topography.

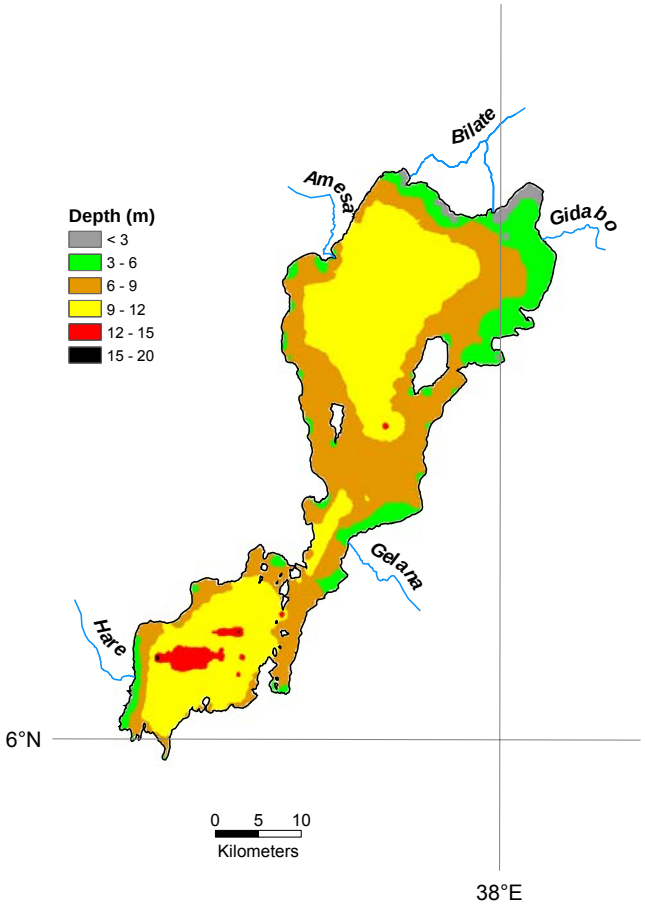

Figure 5.13. Bathymetry map of Lake Abaya.

The bulk of the remainder of the lake is composed of sediment with high fine fraction which indicates the main depositional basin and part of the nearshore zones. The changes occurring in the sediment textural characteristics from a nearshore environment through a zone of mixing associated with decreasing energy to an offshore zone is which the sediments are derived primarily from suspension. These zones representing decreasing energy from nearshore to offshore environment verified by the textural characteristics. The basin sediments are composed of fine grained, soft, sandy-silty-clay, grey black, grey, to reddish brown in colour. Exception is consolidated dark grey between the largest island in the south basin and the east shore and the sheltered zone near west shore in the north basin.

Near the shore line the sediment colour is dark grey to black except the water-sediment interface. A thin oxidized microzone of reddish brown, varying in thickness was observed at the surface of all mud samples. The black grey colour dominates near the east shores of the northern part of the south basin and the north basin, whereas the grey to brown colour is present near the west shore. The reddish brown clay at the most top surface of the recent mud increases towards the centre and south. This increasing reddish brown clay at the top suggests the fine materials derived mainly from suspension are deposited at the low energy zones. The coarsening of the grain sizes can be observed by the decrease of

the reddish brown at the most top at the water sediment interface and darkening of the underlying light grey and brown to black grey onshore.

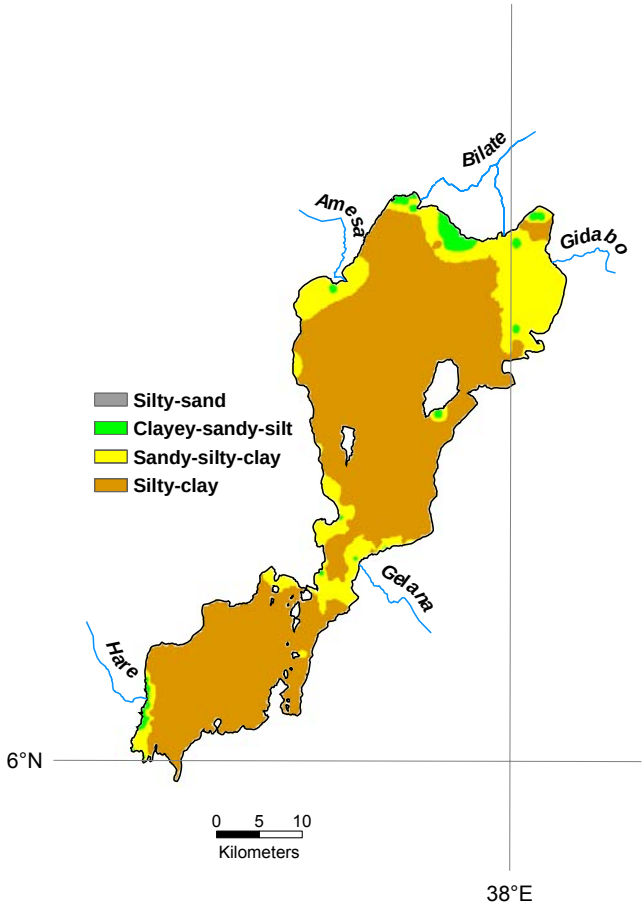

Figure 5.14. Surficial sediment distribution in Lake Abaya.

5.2.2. Sediment composition

The sediments of Lake Abaya contain variable amounts of quartz, feldspar (essentially sanidine and andesine), clay minerals, calcite, and organic and carbonate carbons, with possible traces of hematite, magnetite, pyrite and hornblende in some samples. Hematite and magnetite were often detected in several samples. The presence and absence of these different minerals is a clear function of location. This section presents some data on the horizontal heterogeneity of major chemical and mineralogical components of the lake sediments. The detailed mineralogical composition is given in Appendix A.

5.2.2.1. Quartz

The quartz content is found to be within the range of <1 to 40 percent. With respect to quartz concentrations in surfical sediments, the lake basin may be partitioned geographically (Figure 5.15). Percent content of quartz is high (> 20 percent) in the areas close to the mouths of the major rivers entering the lake in the north basin, except Shope

River where the quartz fraction settled in the flat flood plain before reaching the lake. Although relative amounts of quartz are not significant in most Lake Abaya sediments, they are nevertheless useful indicators of sedimentation patterns.

The influence of major streams in the distribution of sediment in the north basin is illustrated by the fact that sediments of the quartz fraction carried significant distance from the river mouth by flow current before setting. The general trend for horizontal distribution of quartz minerals is decrease to the centre of the main basins and from north to the south. Samples from the south basin contain quartz within 10 percent. It is interesting to note that the main depositional zone of sediments in the north basin contain quartz content in the range of 5 to 10 percent, whereas the south basin has less than 5 percent in the majority of samples both from onshore and offshore. In general, the quartz content of surficial sediments show decreasing tendency towards to the south. Thus, considering the quartz population in Lake Abaya, it is convenient to define the north end as the area of high concentration and the south end as the area of low concentration.

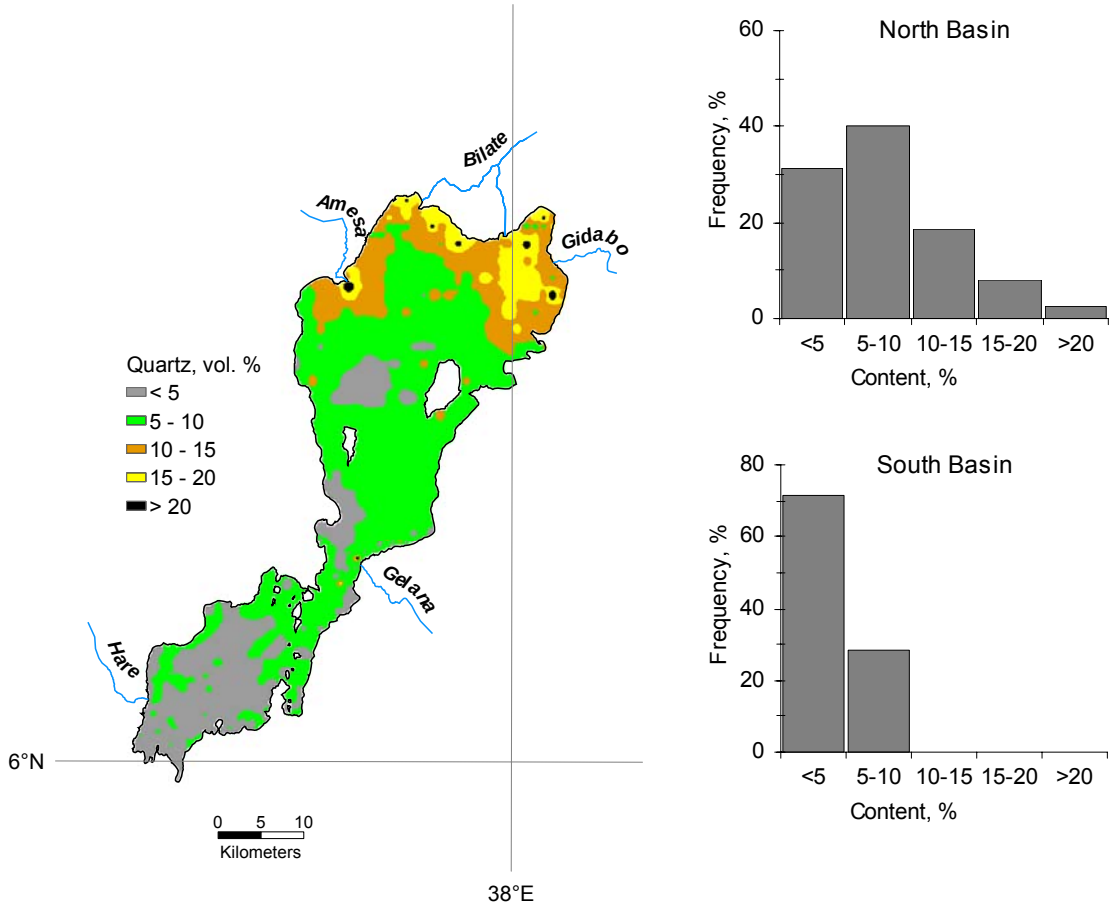

Figure 5.15. Quartz distribution in surfacial sediments of Lake Abaya.

5.2.2.2. Feldspar

One of the most abundant constituent minerals in Lake Abaya sediments is feldspar. All surficial sediments collected from Lake Abaya contain feldspar. However, there is considerable variability (Figure 5.16): relatively high concentrations associated with nearshore sediments and with stream deltas where the winnowing (erosion) action of waves or currents is not effective in preventing deposition of feldspar rich inputs. Thus, distribution of feldspar followed nearly similar patterns in both north and south basins. Lake Abaya sediments contain substantial quantities of feldspar ranging from 3 to 76 percent (overall mean total feldspar of about 28 percent).

Highest feldspar contents (more than 60 percent) are observed along the west and north shorelines near the mouths of major tributaries and the lower feldspar contents occur around the centre of the main basins. The distribution structure at the area of the narrow connection of the north and south basins at the bottleneck parallels that of the nearshore zones. It is important to note that samples taken from the station close to the shoreline but within the influence of cliffs or hilly surrounds have lower feldspar content. The general feldspar concentration is less than 20 percent in the main basin, distribution in the north basin being slightly more variable than in the south basin.

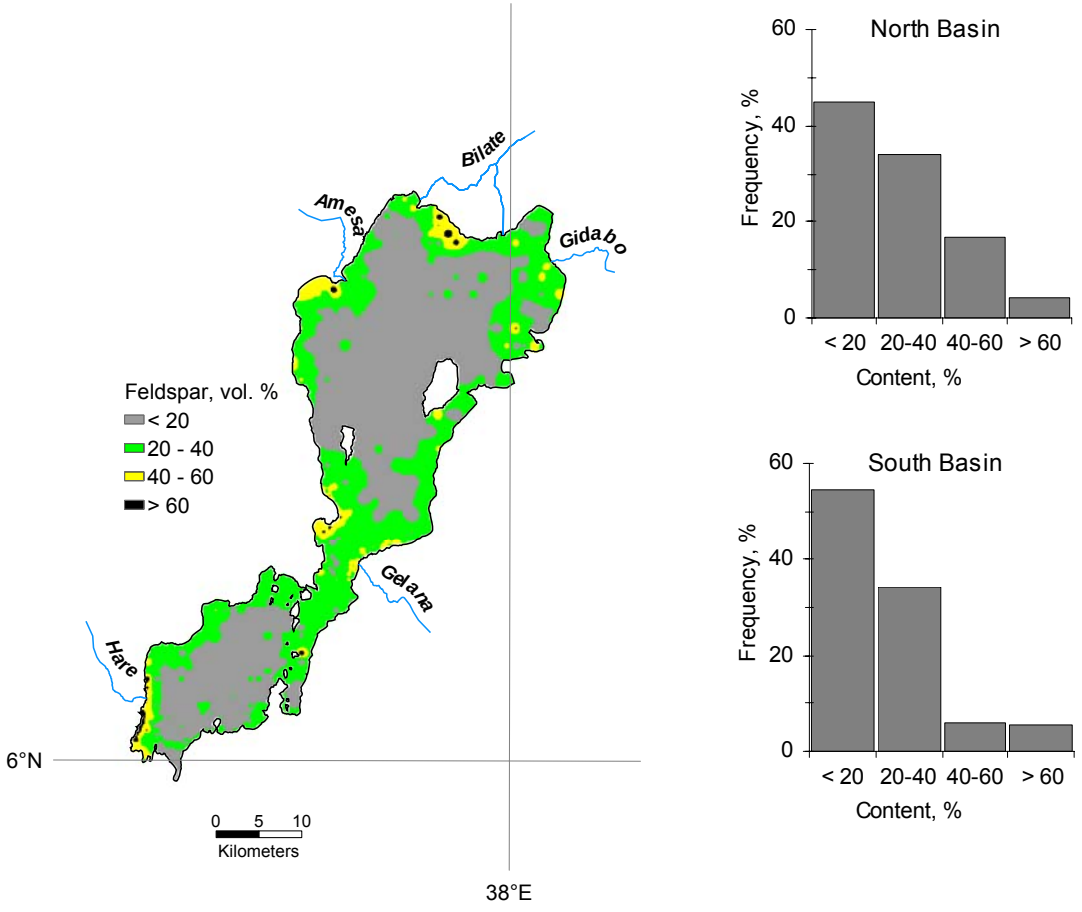

Figure 5.16. Distribution of feldspar in surficial sediments of Lake Abaya.

5.2.2.3. Clay

Total clay minerals distribution in surficial sediments of Lake Abaya is shown in Figure 5.17. Clay minerals are the most abundant mineral fractions in Lake Abaya sediments. Total clay minerals at each sampling site were calculated by subtracting quartz, total feldspar, calcite, organic matter and other traces, if any, of hematite, magnetite, pyrite and hornblende from the total sediments. Organic matter was computed from organic carbon using a factor of 1.72 (Schoettle and Friedman, 1973). Clay content computed from quartz, carbonate, and organic carbon, however, is probably a more precise method which is more desirable for the interpretation of geochemical data (Thomas, 1968).

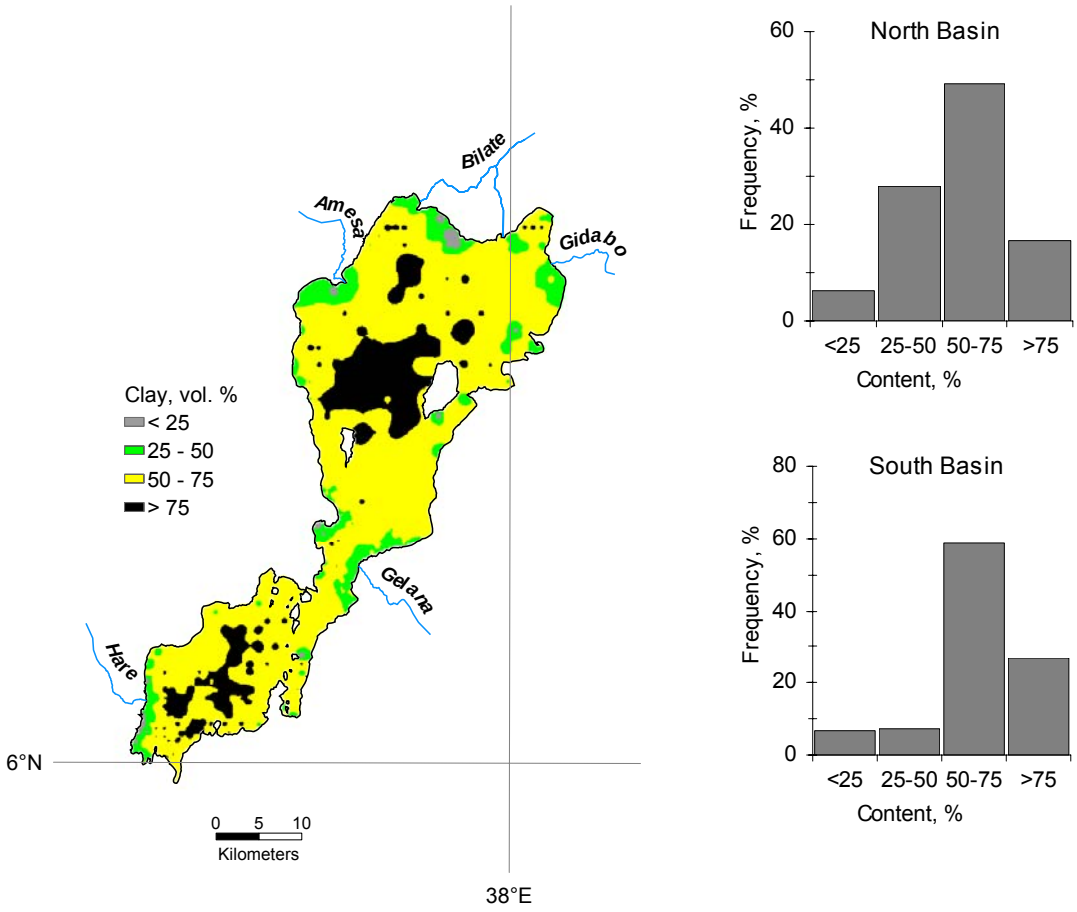

Figure 5.17. Distribution of clay in surficial sediments of Lake Abaya.

Clay mineral content ranges from 6 to 96 percent with a mean of 61 percent. Relatively low concentration of clay minerals is associated with nearshore sediments and stream deltas where the winnowing action of waves or currents is effective enough in preventing deposition of fines. Sediments with less than 25 percent of clay (hence mostly sandy) are restricted to the west shoreline and northernmost part close to the mouth of major rivers (Figure 5.17). Clay minerals show the expected general distribution pattern, with relatively low values in nearshore sediments increasing to maximum concentration at the centres of

the main basins. Further noticeable patterns in clay distribution are: (1) increasing clay concentration in the nearshore sediments collected from stations surrounded by cliffs or hills; (2) generally low clay concentration at the narrow bottleneck transition and narrow passage between the largest Gidicho Island and east shore; and (3) southward increasing tendency.

5.2.2.4. Calcite

The calcite distribution in Lake Abaya is shown in Figure 5.18. Most samples contain only small quantities of calcite, and its amount ranges from less than 1 to 24 percent. Similar distribution patterns are observed in the north and south basins. Calcite is relatively more abundant in the shoreline than in the main basins sediment samples of both north and south basins. No general trend is observable, but higher calcite values occur around narrow passages such as the area of bottleneck connection and to the east of Gidicho Island. Similar amounts of calcite values observed in the west shoreline of south basin.

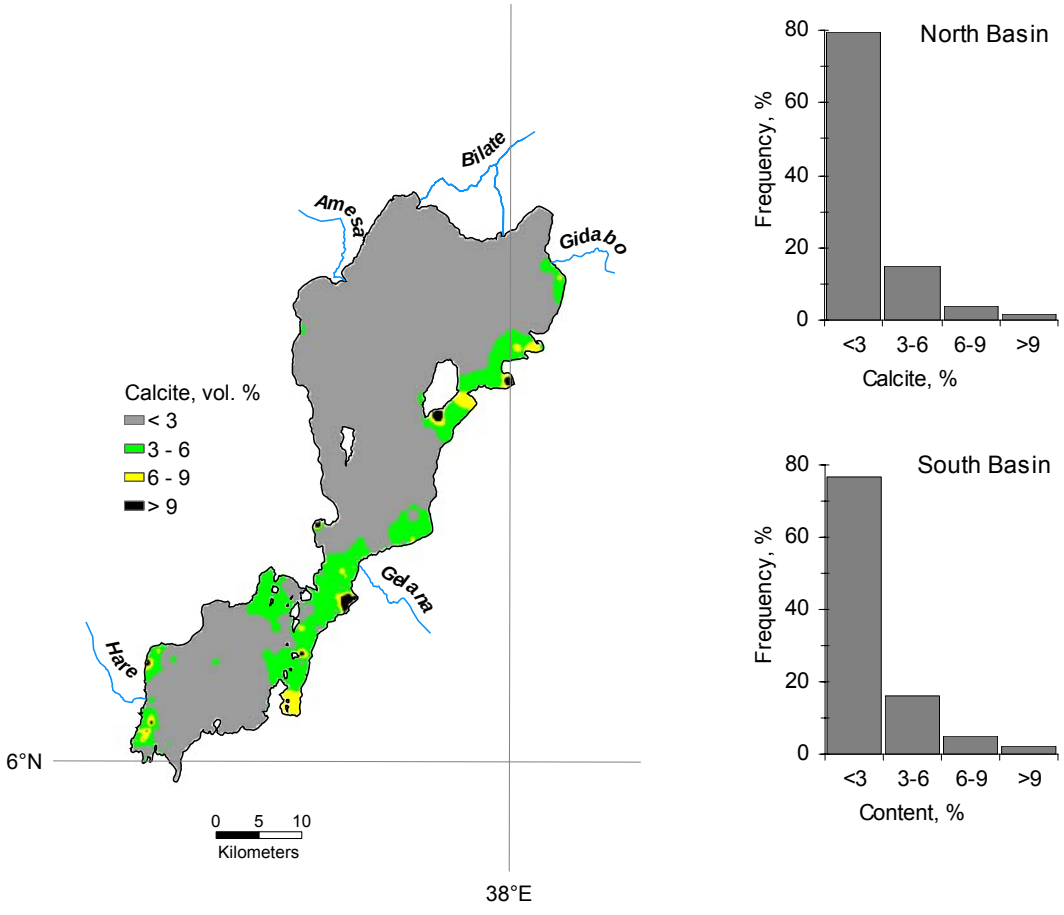

Figure 5.18. Distribution of calcite in surficial sediments of Lake Abaya.

5.2.2.5. Organic carbon

The organic carbon distribution in surficial sediments is shown in Figure. 5.19. Organic carbon is generally low throughout the lake ranging from less than 1 to 16 percent. Few values of organic carbon exceed 3 percent and most of them contain between 0.5 and 1.0 percent in both south and north basins. The highest organic carbon content was observed in the delta of Gelana River. Organic mater is more evenly distributed in the main basin and high organic carbon contents are confined to nearshore zones. It is readily observed from organic carbon distribution (Figure 5.19) that organic muds settled more rapidly close to the input points. A decline in organic carbon to the west is observed around the area of narrow bottleneck transition. Sediments from the western part of the narrow transition were mostly depleted of organic carbon. A marked difference is apparent between the organic sediment distribution in the sediment samples from deltas of the eastern and western major tributaries. Sediment samples from the deltas of eastern major tributaries showed higher relative abundance of organic carbon. Similar amounts were observed in the northern part of the south basin.

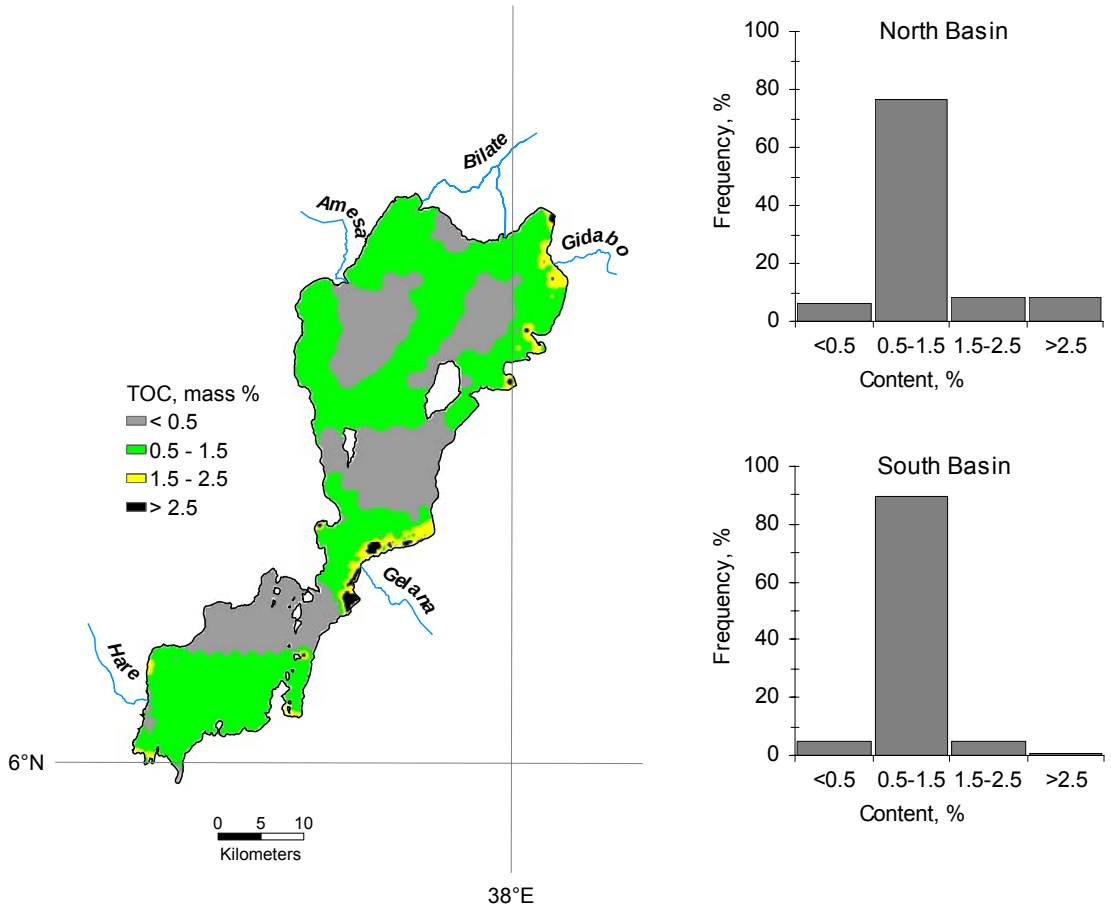

Fig. 5.19. Distribution of organic carbon in surficial sediments of Lake Abaya.

5.2.2.6. *Carbonate carbon*

The distribution of carbonate carbon in the surficial sediments of Lake Abaya is presented in Figure 5.20. Carbonate carbon is generally low throughout the lake ranging from 0 to 3 percent. No general trends observable but higher carbonate carbon values occur along the eastern shoreline and in the bottle neck connection in the middle. Few values of carbon exceed 1 percent and most of the sediments in Lake Abaya contain less than 0.5 percent carbonate carbon. The sediments of the narrows have increased carbonate carbon. From x-ray diffraction results, all the carbonates appear to be in the form of calcium carbonate with no siderite or dolomite resulting parallel distribution pattern with calcite.

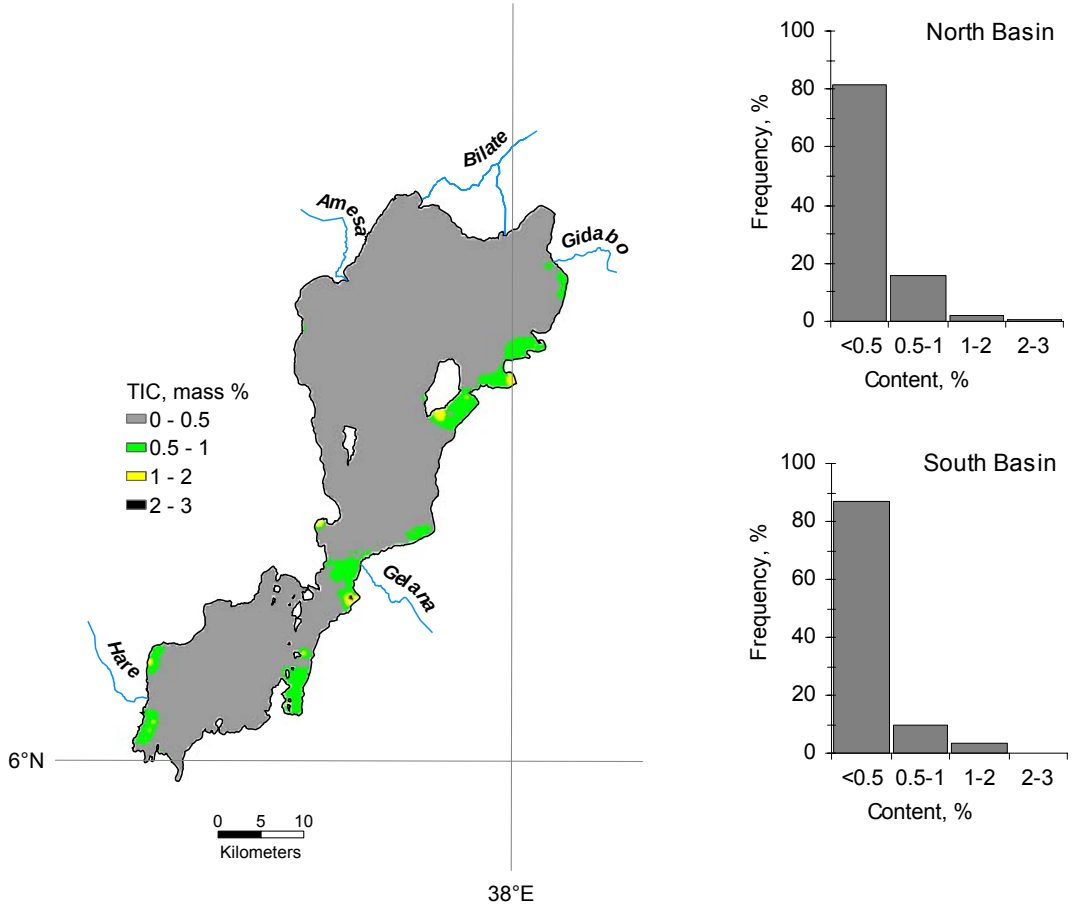

Fig. 5.20. Distribution of carbonate carbon in surficial sediments of Lake Abaya.

5.2.2.7. *Trace minerals*

Trace minerals detected by X-ray diffraction are principally hematite, magnetite, pyrite and hornblende. Widespread traces of hematite occurred in surficial sediments of Lake Abaya (Figure 5.21). The general distribution pattern shows increasing tendency southward. The amount of hematite observed in the north basin is mainly less than 2 percent with occasional occurrence between 2 – 4 percent. It is observed that hematite is an important

constituent of samples from south basin. The distribution in the south basin does not have obvious pattern except increase towards the centre of the basin.

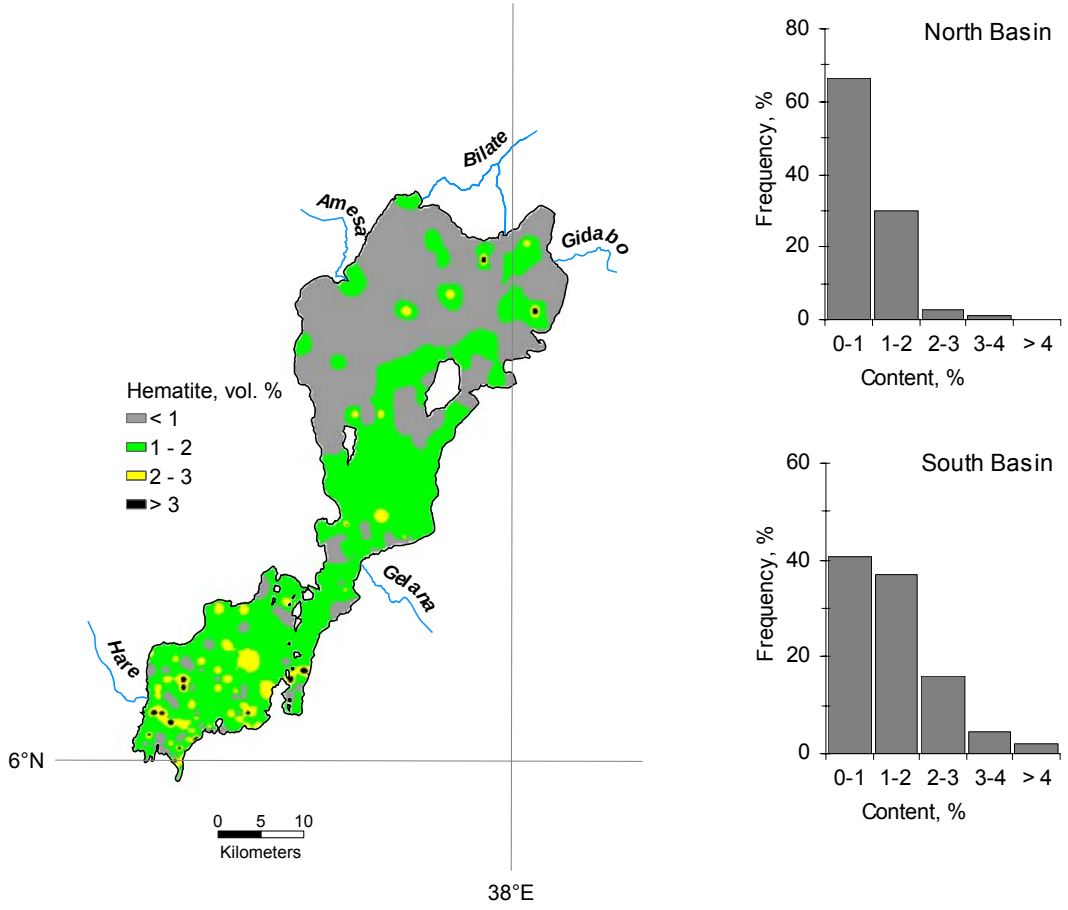

Figure 5.21. Distribution of hematite in surficial sediments of Lake Abaya.

The distribution of magnetite in the surficial sediments of Lake Abaya is presented in Figure 5.22. This distribution, however, is quite variable over the lake basin; increasing tendency towards the mouth of main streams in the western side is evident. It is interesting to note that the maximum concentration is observed in the deepest sampling site in the south basin. Similarly, increasing concentration in the north basin was observed around the deepest zone. Another feature of magnetite distribution is that most of the samples from south basin are found to have magnetite than the counterpart samples from the north basin.

The pattern of spatial variability for concentration of pyrite has some similarity with that of hornblende. Both minerals detected rarely and showed no obvious trend in both south and north basins. Pyrite was detected in more samples from the south basin than from the north basin. The concentration of hornblende also exhibited similar but less pronounced patterns. Larger concentration of pyrite and hornblende are found in the south basin surficial sediments than in surficial sediments of the north basin. The largest pyrite was found near the Hare and Amesa deltas. Like pyrite, the largest concentration of hornblende

was also found in the Hare Delta. On the other hand, pyrite concentrations were substantially smaller (less than 5 percent) than hornblende concentration (5 to 13 percent).

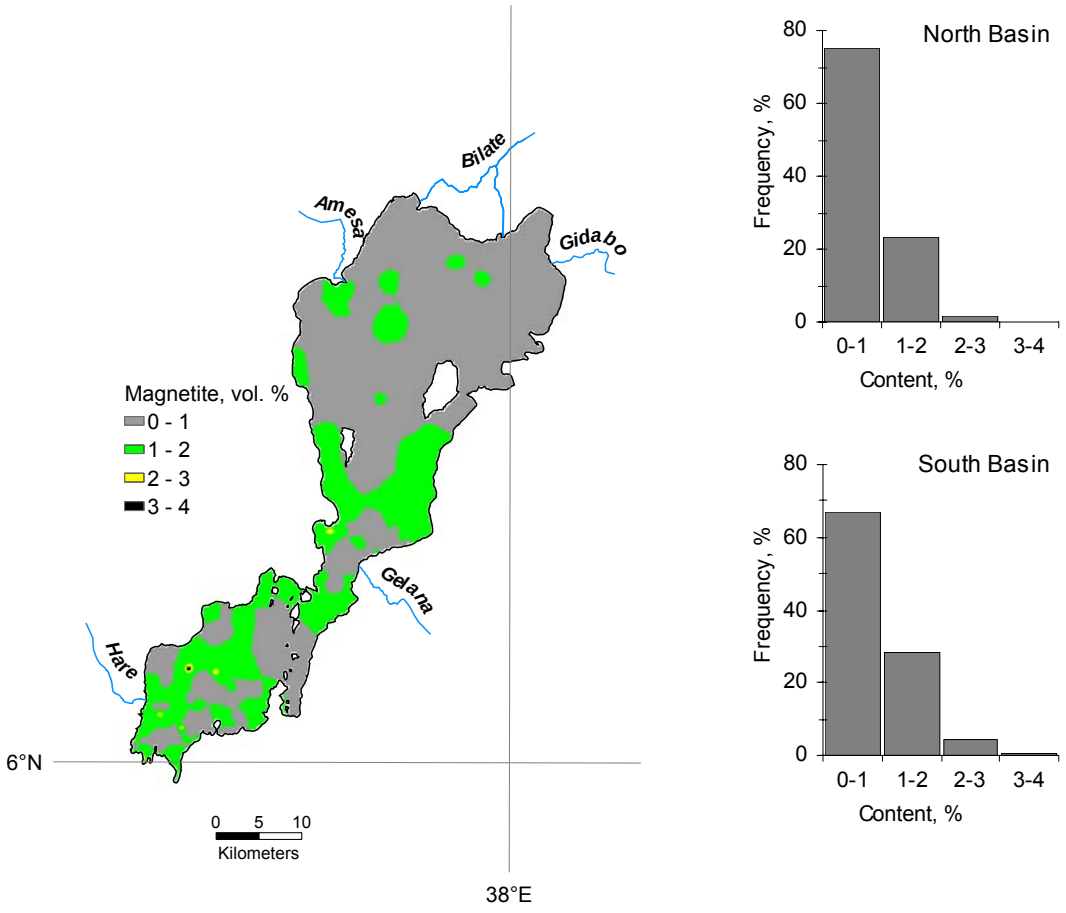

Figure 5.22. Distribution of magnetite in surficial sediments of Lake Abaya.

5.2.3. Interrelationships between variables

A correlation coefficient matrix summarizing the relationships between variables (minerals, water depth) is given in Table 5.10. With 706 samples used in the analysis, a correlation coefficient greater than 0.091 is significant at the 1 percent confidence interval. The expected high degree of relationship between water depth and clay content is obvious from Table 5.10. A comparison of bathymetric contours with the distribution of clay minerals shows that the deeper parts in both basins of the lake are underlain by clay, whereas the shallower parts bottomed by silty sands. Exceptions to this fact are the sheltered near shore regions where reduced circulation by wind allows clay size material to deposit. Clay and feldspar show strong but inverse relationship indicating that high clay content is associated with low feldspar content. It is further demonstrated that feldspar has strong but inverse (or indirect) relationship with depth.

Examination of Table 5.10 shows that with increasing water depth there is a decrease in feldspar, quartz, calcite and organic carbon. Another obvious relationship in Table 5.10 is

direct relationship between calcite and carbonate carbon, as expected. Clay correlated inversely with quartz and calcite.

Organic carbon contents show inverse correlations to depth as discussed previously and direct correlation to calcite, and poor but significant yet inverse correlation to clay. A comparison of lake bottom morphology with organic carbon content and sediment colour shows that interrelationship exists between these variables. The thin sediment deposits of reddish-brown colour at sediment water interface in the shallow parts of the lake are dark-grey to black. In the deeper parts of the lake, sediment colours change to light grey to reddish-brown and the organic carbon content is low.

Table 5.10. Correlation coefficient Matrix

	Quartz	Calcite	Feldspar	Clay	Hematite	Magnetite	Pyrite	Hornblende	TIC	Organic Carbon
Depth	–.366	–.280	–.651	.688	.206	.045	–.155	–.018	–.285	–.317
Quartz		–.129	.048	–.240	–.161	–.247	–.108	–.071	–.139	–.080
Calcite			.208	–.336	.026	.091	.150	.112	.922	.267
Feldspar				–.942	.027	.253	.222	.168	.221	.106
Clay					–.041	–.229	–.286	–.319	–.324	–.224
Hematite						.217	.028	.018	.032	–.058
Magnetite							.099	.129	.046	.020
Pyrite								.219	.183	.125
Hornblende									.081	.064
TIC										.196

Samples from the deltas of the major tributaries contain variable mixtures of clay, quartz, feldspar and calcite and various minerals detected in traces (Figure 5.23). Samples from Amesa, Gidabo and Bilate River mouths have in total higher quartz contents than mouths of others. Traces of pyrite are observed in samples from Amesa and Hare deltas. Feldspar concentrations are highest along the western shoreline; while clay mineral contents are highest in the north and east rivers deltas. Along a transect from west to east there is no clear trend except a more marked increase or decrease of major minerals near shore zones.

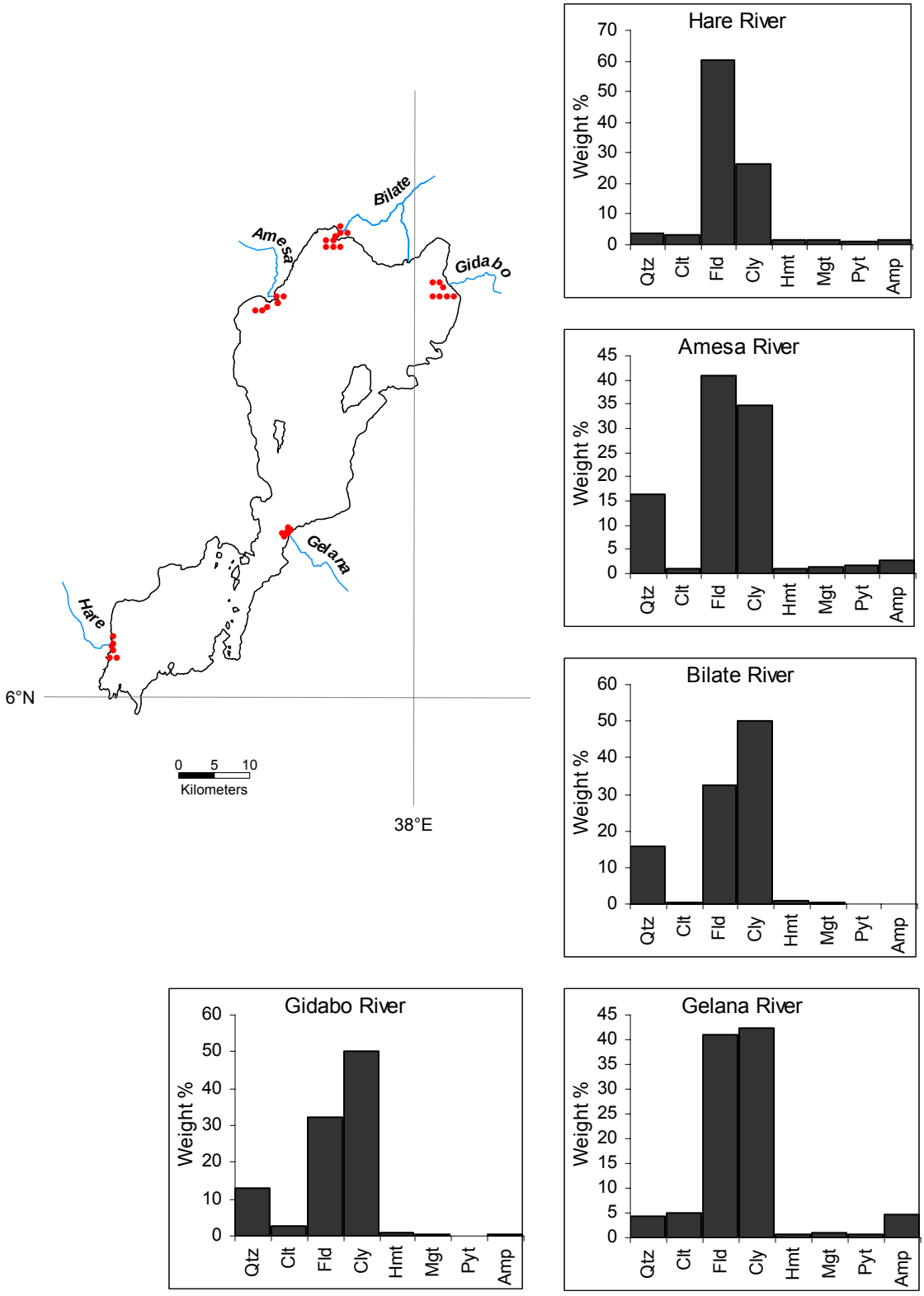

Figure 5.23. Average mineral compositions at deltas of major tributaries.

5.2.4. Cluster analysis

A cluster analysis, using the Ward method, resulted in six groups of sediment samples that differed primarily with respect to their relative mineralogical compositions (Figures 5.24). The main differences between the groups are reflected in the mean percent of the sediment samples (Figure 5.25). The number of samples included in the clusters range between 40 and 239, with minimum and maximum numbers corresponding to clusters 6 and 3, respectively. Feldspar and clay are generally characterized as the most variable minerals across the clusters. All samples included in Cluster 2 from North Basin have above average quartz content. Majority of samples rich in quartz are included in clusters 1 and 2, whereas those rich in calcite, feldspar and hornblende are included in clusters 5 and 6. These samples are located in the deltas of tributaries, while such samples are absent from the central part of the lake basin. By contrast, clusters 3 and 4 mainly occur in samples from the central basin, or are generally characterized by highest values of clay and lowest values of feldspar, quartz, calcite and hornblende.

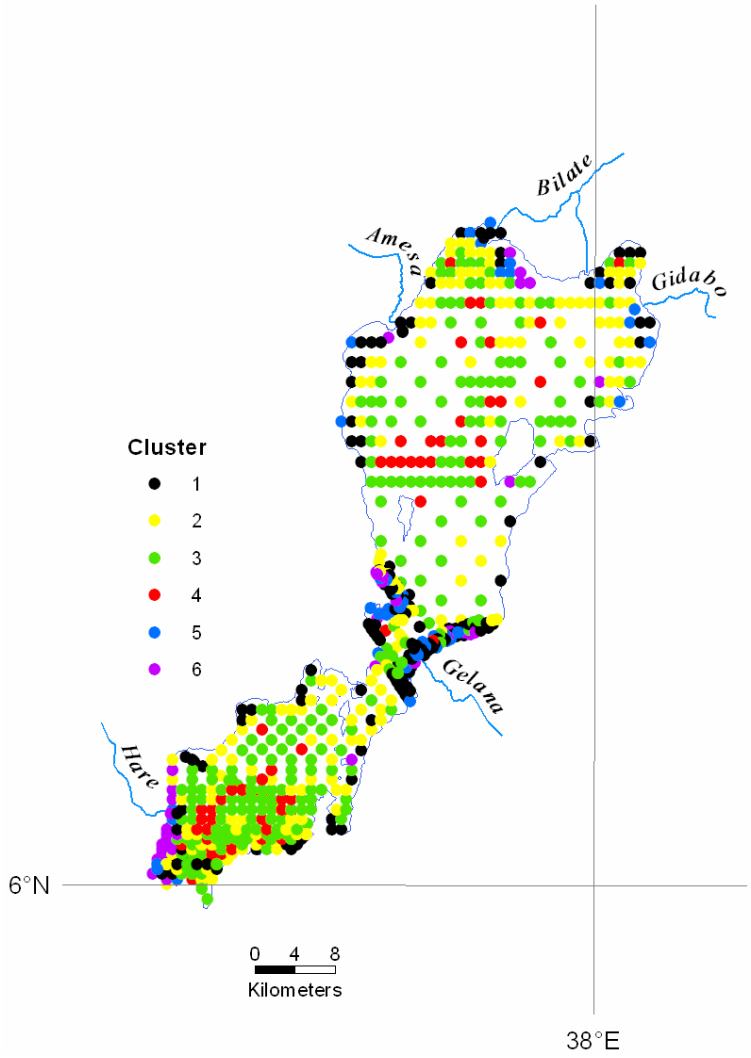

Figure 5.24 Clusters of sediment samples distinguished on the bases of relative mineralogical contents.

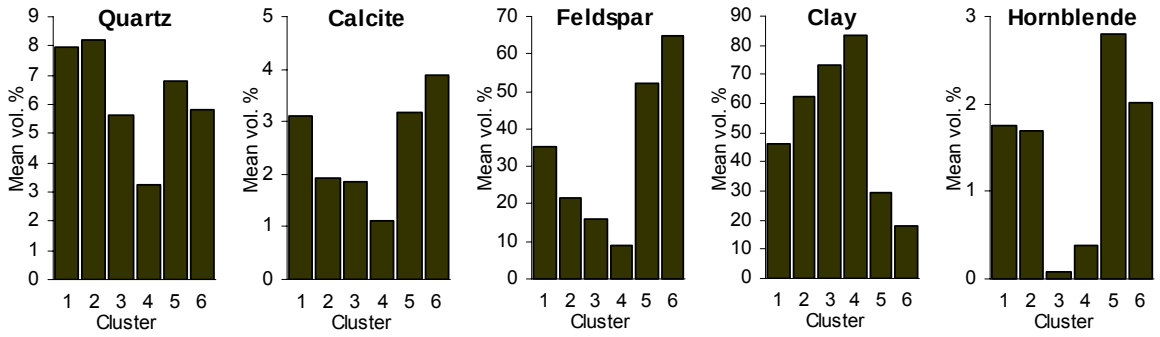

Figure 5.25 Average mineralogical contents of identified clusters.

5.3. Water Quality

5.3.1. Water Temperature

Water temperature at fixed stations in Lake Abaya varied from 21.9^{o}C to 30^{o}C, with an overall average of 24.1^{o}C (*n* = 571). The minimum water temperature at all fixed monitoring stations observed in late June and July 2004 field sessions when stations were visited at different times between 1000 and 1700 local standard time (LST), whereas the maximum temperature measured near-surface in various months when the stations were monitored in the afternoons (Figures B1, B2 and C1, Appendixes B and C). In fact, the time of sampling of the depth profile did not necessarily capture the daily extremes. Because of the high irradiance and the low river inflow during the study period, the lake water commonly attained temperature >20^{o}C throughout the lake. However, it is more likely that the overall cooler temperature of the lake in June and July 2004 than other months from March through October 2004 was determined by a combination of temperature of inflows as well as climatic factors.

Contour plots of temperature profiles at fixed monitoring stations shown in Figures B1 and B2 displayed at bimonthly and monthly sampling intervals for the stations located in the south and north basins, respectively. It is sown that the temperature vitiations in the water column were small. Further, the well mixed conditions from near surface to near bottom, which prevailed during most of the field sessions, are indicated by the nearly vertical isolines. Thus, given its shallow depth and prevailing diurnal wind structure, the Abaya Lake water exhibited very weak thermal stratification, amounting an average temperature differential of about a quarter of a degree per meter positive upwards.

Temperature variations occurring near-surface were confined to the top layer of about 2m thick (Figures B2 and B3). The near-surface water temperature associated with each of the depth-profile measurements indicates that the lake water was warmer in the afternoon by up to 5^{o}C than at 1-m depth when the prevailing wind was light. This was documented by the maximum variation between near surface and 1-m depth observed on 19 May 2004 (Julian day 140) around 1500 LST at station S6 in the north basin when variable winds less than 2 ms^{-1} (and more than 70 percent of the 5-min interval records being less than 1 ms^{-1}) at Wajifo Weather Station prevailed until the sampling time.

To examine the relation between weather and temperature in the lake, the air temperature records at Wajifo Weather Station during sampling dates from the nearest stations S7 and S4 in the north and south basins, respectively, were considered. Since the depth-profiles taken only once during each sampling session were not adequate to examine closely the relation between temperature in the lake and air temperature, 5-minute interval air temperature readings were smoothed with the recent 1-hour records before taking depth profiles. The corresponding average of air temperature records from Wajifo Weather Station were plotted with the average of near-surface and 1-m depth water temperature (Figure 5.24). It is indicated that the fluctuations in the average water temperature nearly parallels the recent 1 hour averages of 5 minute interval air temperature records, water temperature being warmer than air temperature when measurements were taken before noon.

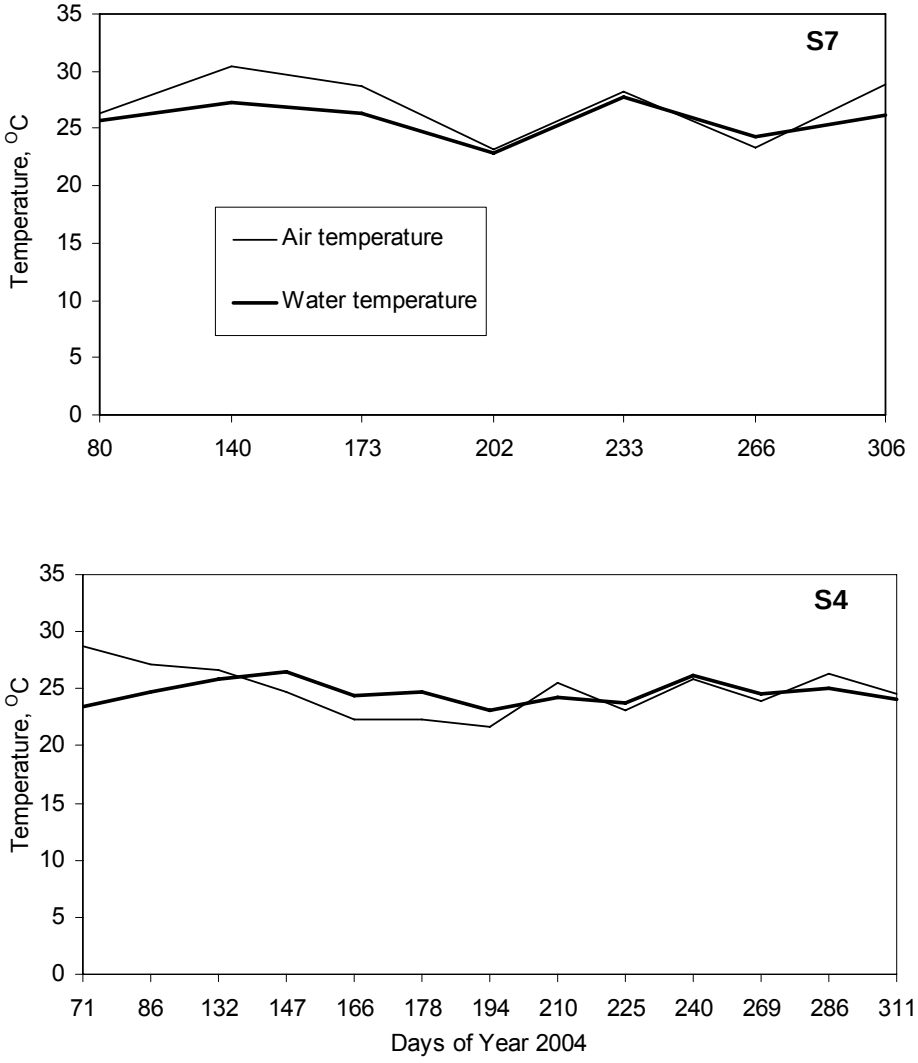

Figure 5.24. Comparisons of daily average temperature at Wajifo Weather Station and near surface water temperature at nearest fixed stations from south (S4) and north (S7) basins.

The water temperature averaged over the water column at fixed monitoring stations during the sampling days of Year 2004 and the corresponding monthly averages of air temperature records at Wajifo Weather Station were shown in Figure C1. Average temperatures ranged between 22.2 and 27.2 (n = 75). In general, temperature in Lake Abaya exhibits weak seasonal signals, the successive bimonthly and monthly averages of depth profiles in the south and north basins, respectively, varying up to 4.8^{o}C and 2.2^{o}C. Further, nearly similar trend of the monthly averages between fixed monitoring stations were found. On the other hand, the spatial variability of up to about 5^{o}C was measured on a given sampling date between about 1000 and about 1600 LST at the same water depth. Such differences that appear to be spatial because of change in value from one station of the lake to another can be temporal due to the time taken to travel between the monitoring sites.

5.3.2. pH

The values of pH at fixed monitoring stations in Lake Abaya ranged from 8.8 to 9.3 (overall mean = 8.9, n = 571). The maximum pH value of 9.3 was observed in the north basin on Julian days 79 and 80 at stations S5 and S7. Other stations monitored on the same dates had values of 9.1 and 9.2 at stations S6 and S8, respectively. Thus, when high pH values were observed, it was common to measure them at most of the station in the lake. Bimonthly measurements of pH values exceeded 9.0 only on Julian day 147 (around the end of May) field session in the south basin. The lowest values of pH observed at stations close to the mouth of major tributaries. The depth profile data shown in Figures B7 and B8 indicate that vertically homogenous pH value occurred mostly, or that condition near the surface can be different from other measurements by 0.1 unit increment occasionally. Further, horizontal spatial structure on a given sampling session is virtually absent.

The monthly and bimonthly measurements at fixed monitoring stations were analysed for the frequency distribution of pH values. Results for March through October 2004 demonstrated that an excursion into pH value greater than 9 units was a relatively rare event (about 7 % when all stations and depths combined). Another remarkable feature of the profile data is the geographical dependence of the frequency distribution pH values. The pH value of the largest percentage of the data (more than 80%) were observed to be not greater than 8.9 at stations situated close to the mouths of the major tributaries.

5.3.3. Conductivity

Water conductivity at fixed monitoring stations in Lake Abaya ranged from 861 to 1162 μScm^{-1} (overall mean = 1124 μScm^{-1}, n = 571). The minimum conductivity was observed at station S2 on Julian day 286 (around mid of October), whereas the maximum conductivity observed at station S4 on Julian day 240 (around end of August). Except for one field session mentioned above, conductivity at station S2 was found to be high (>1110 μScm^{-1}). Conductivity in the south basin stations generally exceeded those of the stations in the north basin. During the study period, conductivity differentials of the depth profiles at fixed stations amount about 40–296 μScm^{-1} in the south basin, and about 30–119 μScm^{-1} in the north basin. There is no clear seasonal signal in conductivity at fixed stations other than

specific and marked decline at stations close to the mouth of main tributaries. Conductivity near surface displayed lower values at stations S1 and S2 in the south basin during Julian day 286 sampling event (Figure B3).

The depth profiles structure of conductivity at fixed stations shown in Figures B3 and B4 are obscured because there is such relative constancy or noisy character in conductivity. Overall, the higher frequency (> 90 percent) of water conductivity was greater than 1100 μScm^{-1}. It is shown in Figure C2 that the average conductivity distribution is predominantly a north-to-south gradient of increasing conductivity. Time related variation of the average conductivity at fixed stations in the north basin showed gradually increasing trend, whereas stations in the south basin exhibited initially high levels decreasing until Julian day 132 (around mid May), gradually increasing until Julian day 269 (around end of September, then gradually decreasing (Figure C2).

5.3.4. Dissolved Oxygen

Dissolved oxygen in water column at fixed monitoring sites was found to be in the range of 5.4 - 7.9 $mg.L^{-1}$ (mean = 6.8 $mg.L^{-1}$, *n* = 571). An overall analysis of the depth profile reveals that a large percentage of the data (about 75 percent) is made up of concentration of dissolved oxygen (DO) greater than 6.5 $mg.L^{-1}$, and concentrations less than 6.5 $mg.L^{-1}$ did not appear before Julian day 240 (around end of August) at site S1, or even not before October at other stations (Figures B5 and B6). The minimum value of DO was observed at station S2 on Julian day 286 (around mid October) near surface and at station S9 on Julian day 306 at 0.5m and 1m depths above the lake bed, whereas the highest value obtained on Julian day 71 (March) at station S3. In general, the content of dissolved oxygen fluctuated mostly (> 90 percent) in the range of 6-8 $mg.L^{-1}$ in the depth-profile dataset, and occurrences of dissolved oxygen values less than 6 $mg.L^{-1}$ were rare during the study period.

The vertical stratification is rare and slight as shown in Figures B5 and B6, the maximum gradient amounting on the order of 0.1 ppm/m increasing uniformly upward. In general, vertical variation in dissolved oxygen was insignificant; and a relatively slight stratification in DO observed in deep water. Even little variations in the vertical structure of DO are found to be confined to the top 1 m layer of the water body. There is no apparent correlation with depth in stratification, although low DO events occur primarily in the measurements at depth. Occasional profiles show uniform DO throughout the depth. General trend of slightly declining DO concentration occurred starting July, 2004.

Figure C3 shows mean values for dissolved oxygen obtained from depth profiles measured once at each site during regular field sessions around between 0830 and 1500 LST in the south basin and around between 0930 and 1730 LST in the north basin. Mean dissolved oxygen of each sampling event was found to generally high throughout all fixed sites. There was slightly different time-related variation of DO between south and north basins. In the south basin, initially high levels decreased until Julian day 132, increased on Julian day 147 and staid nearly constant at that level until Julian day 194, then decreased gradually. On the other hand, the north basin average DO values stayed constant until Julian day 173, then gradually decreased at constant rate in the remaining sampling sessions. The mean of overall profile data at each fixed station also indicates that average dissolved

oxygen concentrations at fixed monitoring sites are uniformly high (Figure C3). Exception to this is the average of two measurements taken at station S9 which showed slightly lower dissolved oxygen mean.

5.3.5. Suspended solids

Water column profile of total suspended solids (TSS) concentrations in Lake Abaya at fixed monitoring sites observed to have great variability in the range 4 – 404 $mg.L^{-1}$ (overall mean = 77 $mg.L^{-1}$, n = 327) during the study period. The average concentration of the TSS from the south basin was 50 $mg.L^{-1}$, n = 208, and from the north basin 123 $mg.L^{-1}$, n = 119, whereas the maximum concentrations were 181 $mg.L^{-1}$ and 404 $mg.L^{-1}$ for the stations in the south and north basins, respectively.

Suspended solids in Lake Abaya have a close geographical association with regions of inflow and stations remote from river inputs. The depth profile dataset revealed that the maximum total suspended concentration was observed at station S9, whereas the minimum concentration was observed at station S6 at a depth of 1m above the lake bed. Overall, TSS concentrations were higher at stations close to major tributaries, as expected. On the other hand, maximum range of station values observed at stations S2 and S7 in the south and north basins, respectively, whereas the minimum ranges of station values found at station S9 in the north basin and station S4 in the south basin.

Stratification in TSS is usually noisy, especially at stations located in the deeper central parts (Figures B9 and B10). Few samples taken from fixed sites S8 and S9 in the north basin displayed higher, but nearly homogenous TSS concentrations. This is no doubt due to the riverine inflow containing high proportion of fine grained particulates. It is important to note that significant concentrations of TSS found in samples taken from various depths at stations situated far away from main tributaries and central parts of the lake. This suggests that fine sediments that easily maintain in suspension account for most of the material carried by the river and are largely transported as suspended sediment.

The most remarkable feature of TSS observed during this study is more frequent occurrence of low TSS concentrations near the bed than near water surface at deeper sites. Figure 5.25 presents comparisons of TSS concentrations found at three depths (near surface, at 2 m water depth, and at 1m above the bottom) on sampling days of Year 2004. The highest frequency (about 67 percent of sampling sessions) of occurrence of higher TSS concentration near surface than near bed were found at deep and central station in the south basin (S4). At the same site, samples taken from 2m depth had more frequent (about 73 percent) occurrence of higher concentrations than samples taken 1m above the lake bed. In the central part of the north basin, stations S5 and S6 had equal frequency (50 percent) of occurrence of higher TSS concentrations near surface than near the bed.

Averages of depth profiles indicate the relative importance of inputs from different main tributaries (Figure C4). Graphs corresponding to stations in the south basin show erratic and complicated changes of bimonthly variations in average TSS concentrations. It is interesting to note that the general trend at station S5 in the north basin parallels the averages of stations S6 and S7 upstream. Because station S7 is mainly influenced by Amessa River input, other main tributaries have a modifying effect to station S5

downstream. Further, the declining trend during the initial bimonthly sampling sessions at station S4 in the south basin nearly parallels the general trend of the nearest monthly sampling station S5 in the nearest sampling date in the north basin.

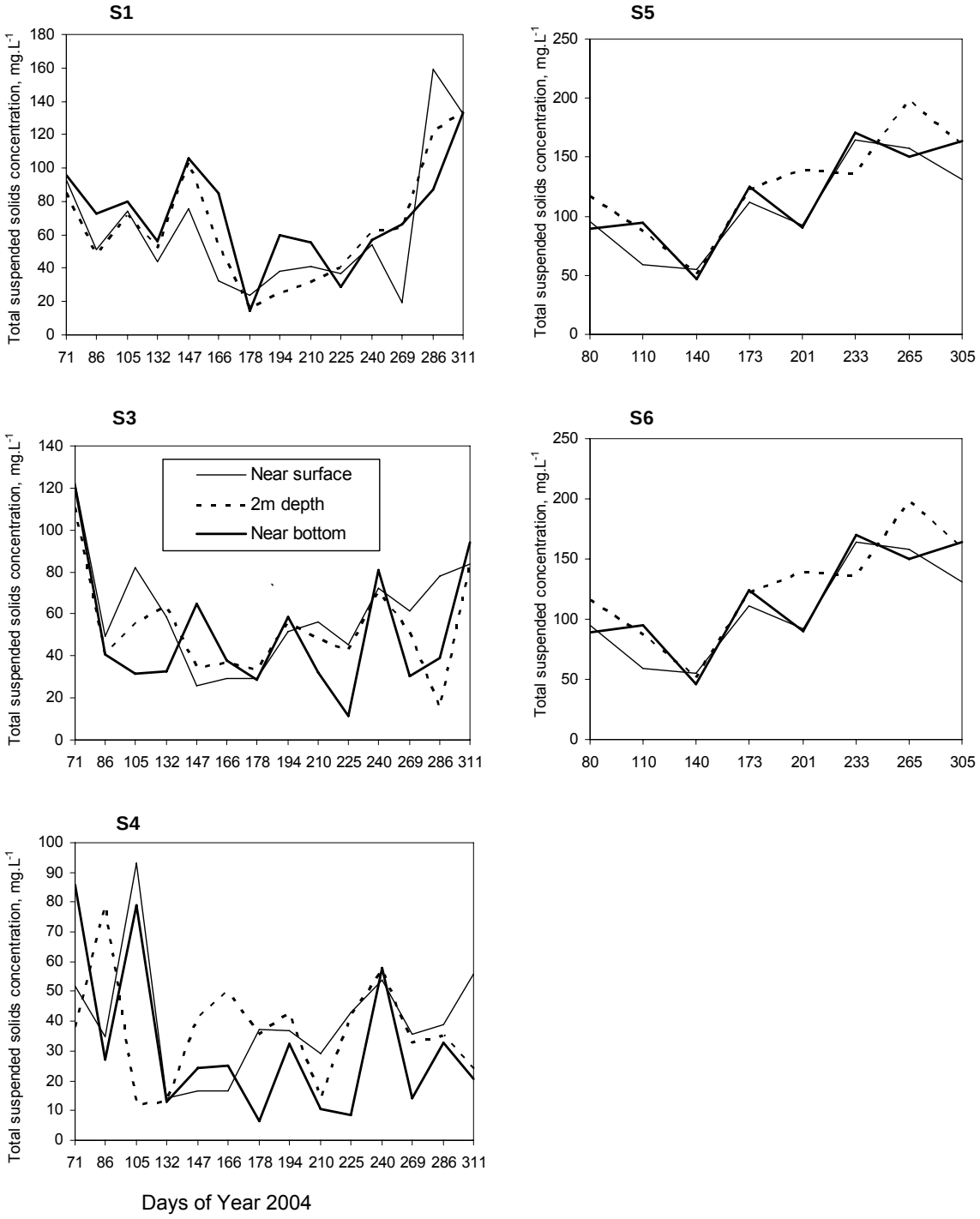

Figure 5.25. Comparisons of total suspended solids concentrations at three depths during sampling days of Year 2004.

5.3.6. Dissolved solids

Total dissolved solids (TDS) concentrations obtained from some water samples taken from fixed monitoring sites in Lake Abaya range 618 – 1206 mg.L^{-1} (mean = 872 mg. L^{-1}, *n* = 193). The maximum and minimum TDS concentrations depth profiles were observed in October 2004 during different field sessions at stations S4 and S9 in the south and north basins, respectively. Like TSS concentrations, no obvious vertical stratification was observed, and occurrences of higher TDS near surface than near lake bed were also common (Figures B11 and B12). The range of the TDS concentrations at fixed stations showed maximum values at S4 and S6 in the north and south basins, respectively, whereas the corresponding minimum values were found at stations S1 in the south end of the lake and at station S8 at the north end and close to the mouth of the largest tributary.

Mean TDS concentrations at fixed stations show that monthly data from north basin were more variable between sampling sessions than bimonthly data from the south basin (Figure C5). A close look at the mean data structure revealed nearly uniformly constant mean TDS concentration appeared from Julian day 132 through 225 at station S1, whereas gradually decreasing trend observed in other fixed sites in the south basin during the same time period. Exception to this is TDS starting to increase at stations S3 and S4 after sampling session on Julian day 194. This trend is followed by uniformly increasing trend in all fixed sampling sites, reaching the maximum values of about 1116 mg.L^{-1} at station S2, and 1190 mg.L^{-1} at station S4 during the rest of the sampling sessions. Although there is no systematic variation between sampling sites in the north basin, the general variation between sessions followed similar fashion. Another spatial structure of the TDS concentration was that overall averages are higher at stations situated far away from the mouths of major tributaries.

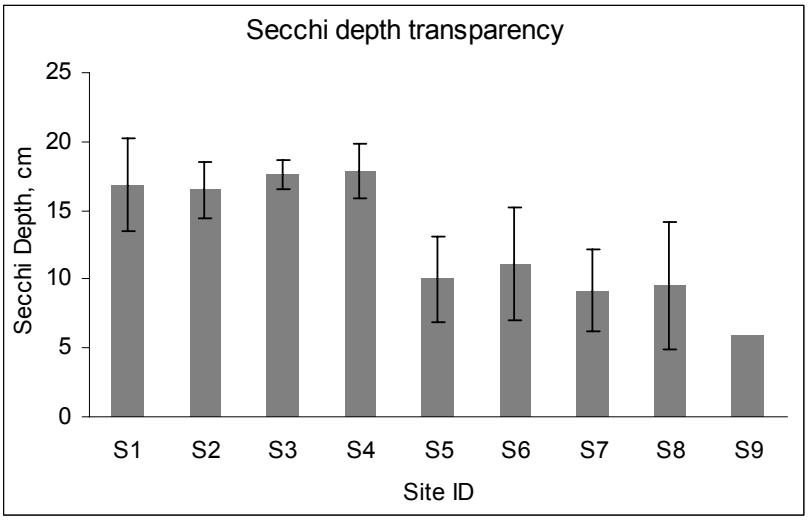

Figure 5.26. Average Secchi depth transparency (±SD) at fixed monitoring stations (see Figure 4.4).

5.3.7. Secchi depth distributions

Water transparency (Secchi) at fixed monitoring stations in Lake Abaya was found to be extremely low with Secchi disk depth average of 15 cm (range 5–20 cm, *n* = 71). The maximum transparency was observed at station S4 situated at the central part of the south basin, whereas the minimum Secchi value was measured at station S8 close to the mouth of the largest tributary. However, the difference in Secchi disk readings between shallow sites, which are close to the river mouths and shorelines, and central deep parts of the lake during sampling dates has been less than 5 cm. Exception is significantly lower transparency further south, at station S1. Overall data structure of the routine measurements at fixed monitoring stations is that there has been little variations between sampling sessions and no significant trend in the south basin, whereas the north basin showed decreasing transparency with time. It is clear from Figure 5.26 that station mean values in displayed increasing transparency from single measurement taken from station S9 in the northeast to stations S3 and S4 in the south basin (mean Secchi 18 cm, *n* = 12).

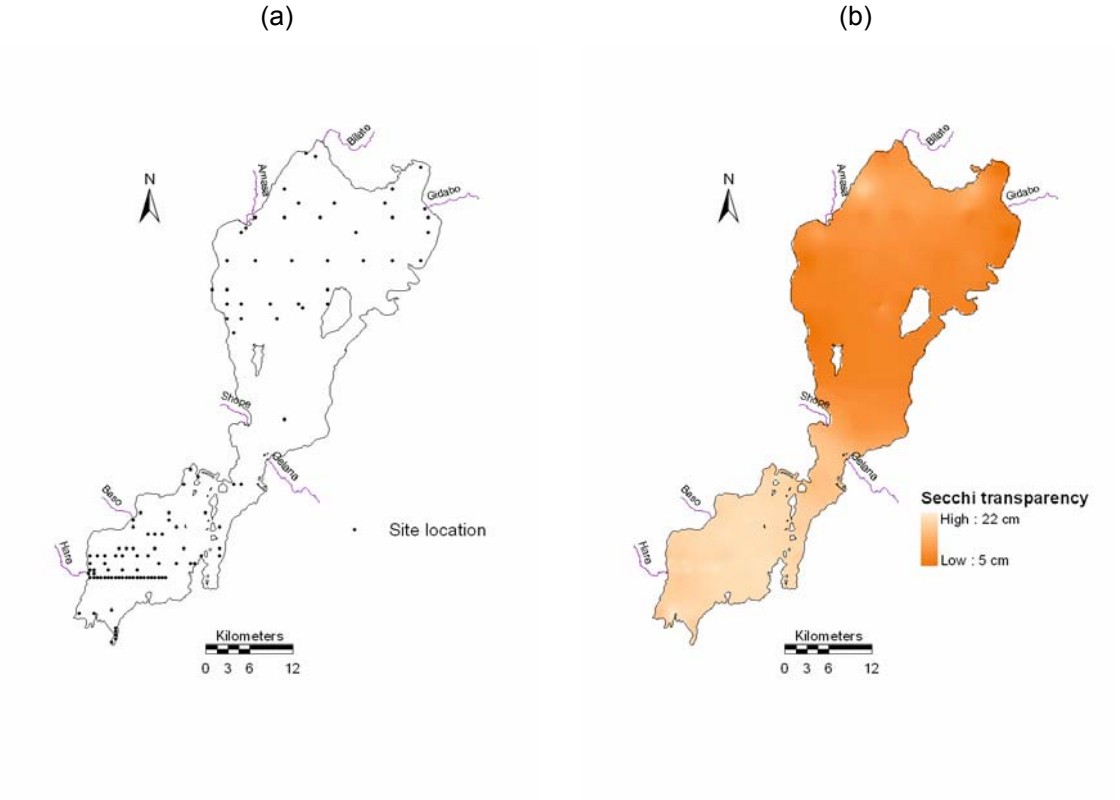

Figure 5.27. (a) Secchi depth measuring sites location, and (b) spatial distribution of Secchi Disk Transparency.

The mean Secchi values at fixed monitoring sites were combined with single measurements taken from some sediment sampling locations (Figure 5.27a) to estimate the mean spatial distribution of water transparency (Figure 5.27b). Comparison of individual Secchi values with their 'site mean' for the survey period indicates that most of the measurements vary within 3 cm above or below the site mean value. Thus, the visual

impression given in Figure 5.27b, and derived from combined dataset, provides good estimate of the spatial variation of transparency throughout the lake. Figure 5.27b shows that there is a clear increasing transparency to the central parts and southwards overall. Figure 5.27b also revealed that there was better clarity at the northwest in the north basin close to the cliff and hilly surrounding boundary.

5.3.8. Interrelationship between quality parameters

To observe statistical differences of water quality parameters between fixed stations, an independent samples two-tailed t-test at a significance level of 0.05 was used to determine if the water column was homogenous for each parameter (Table 5.10). Of the six quality parameters, only water temperature showed significant differences between near surface and near bottom at stations S3 and S4 in the south basin as well as when all stations combined.

Table 5.10. T-test Comparing Near Surface versus Near Bottom Water Quality Parameters at Each Fixed Stations and All Stations Combined.

PARAMETER	S1	S3	S4	S5	S6	S7	All Stations
Temperature	0.094	0.018	0.031	0.102	0.057	0.115	0.000
Electrical Conductivity	0.603	0.646	0.452	0.818	0.640	0.870	0.990
pH	0.331	0.764	0.898	0.929	0.921	0.954	0.608
Dissolved Oxygen	0.421	0.254	0.105	0.473	0.466	0.577	0.169
Total Suspended Solids	0.530	0.352	0.333	0.711	0.761	0.968	0.964
Total Dissolved Solids	0.701	0.700	0.885	0.895	0.846	0.729	0.928

Table 5.11. One-Way ANOVA for Depth Profiles Combines at Stations

PARAMETER	F Value	Significance Level
Temperature	9.808	0.000
Electrical Conductivity	26.909	0.000
pH	7.778	0.000
Dissolved Oxygen	1.839	0.104
Total Suspended Solids	65.683	0.000
TDS	1.392	0.229

Table 5.12. Matrix of Tukey HSD Multiple Comparisons Probabilities.

PARAMETER	S1 v. S3	S1 v. S4	S1 v. S5	S1 v. S6	S1 v. S7	S3 v. S4	S3 v. S5	S3 v. S6
Temperature	0.966	0.936	0.015	0.001	0.157	1.000	0.074	0.004
Electrical Conductivity	0.026	0.001	0.010	0.026	0.046	0.991	0.000	0.000
pH	0.999	0.956	0.001	0.876	0.895	0.997	0.000	0.579
Dissolved Oxygen	0.215	0.911	0.637	0.194	1.000	0.542	0.992	1.000
Total Suspended Solids	0.502	0.000	0.000	0.998	0.000	0.020	0.000	0.200
Total Dissolved Solids	1.000	0.717	1.000	0.975	0.882	0.584	1.000	0.953

PARAMETER	S3 v. S7	S4 v. S5	S4 v. S6	S4 v. S7	S5 v. S6	S5 v. S7	S6 v. S7
Temperature	0.018	0.034	0.001	0.007	0.983	0.000	0.000
Electrical Conductivity	0.000	0.000	0.000	0.000	0.997	1.000	0.999
pH	0.968	0.000	0.199	0.995	0.024	0.000	0.326
Dissolved Oxygen	0.641	0.497	0.497	0.997	0.983	0.919	0.596
Total Suspended Solids	0.000	0.000	0.000	0.000	0.000	0.000	0.000
Total Dissolved Solids	0.882	0.992	0.992	0.266	0.967	0.904	0.559

A one-way ANOVA was used to assess differences between quality parameters among different fixed sampling stations (Table 5.11). Results of one-way ANOVA revealed that only DO and TSS did not differ significantly ($P > 0.05$) from each other. Tukey's multiple comparison test was used to detect significant differences in the parameters among the fixed monitoring sites considered (Table 5.12). Comparisons between sites in the south basin (S1 versus S3) and (S3 versus S4) showed the least number of differences (one), while S1 and S4 in the south basin versus S5 in the north basin showed the greatest number of difference (four).

A summary of the relationship between depth-profiles of water quality parameters measured at fixed sampling stations is given in the Pearson Correlation coefficient matrix in Table 5.13. With 571 in situ measurements of water quality parameters, 327 total suspended sediment and 200 total dissolved solids concentration values, water temperature correlated antipathetically, whereas electrical conductivity and total dissolved solids correlated sympathetically with depth. This relationship is an expression of decreasing temperature and increasing salinity with depth, as expected. On the other hand, total suspended solids correlated antipathetically with depth, describing decrease in total suspended solids with depth. This could be attributed to high proportion of fine clay

particles that could maintain is suspension contained in the sediment input from upland catchments by tributary rivers. Additionally, dissolved oxygen correlated antipathetically and very similarly with total suspended and dissolved solids, and that might be explained by increased biochemical oxygen demand with concentration levels of the constituents both in suspension as well as in solution.

Table 5.13. Correlation coefficient matrix. $^{n.s.}$ denotes not significant, * denotes significant at the 0.05 level, ** denotes significant at the 0.01 level

	Temperature	Electrical Conductivity	pH	Dissolved Oxygen	Total Suspended Solids	Total Dissolved Solids
Depth	–.318**	–.141*	.063$^{n.s.}$	–.067$^{n.s.}$	–.297**	.166*
Temperature		–.185**	.024$^{n.s.}$	–.134**	.109$^{n.s.}$	–.060$^{n.s.}$
Electrical Conductivity			.097$^{n.s.}$	.251**	–.391**	.347**
pH				.236**	–.144*	.059$^{n.s.}$
Dissolved Oxygen					–.178**	–.385**
Total Suspended Solids						–.158*